Enhancing high-frequency axion searches with quantum sensors at RADES

David Díez Ibáñez

Laboratoire de Physique de l'École Normale Supérieure (LPENS)
École Supérieure de Physique et de Chimie Industrielles (ESPCI)

On behalf of **RADES** collaboration

Proposed solution for strong CP problem: not observed charge and parity violations in strong interactions, as it is predicted by SM.

Axions:

- Appear in Pecci Quinn solution to the strong CP problem
- Viable dark matter candidate

Viable dark matter candidate.

Conversion into photons via inverse Primakoff effect:

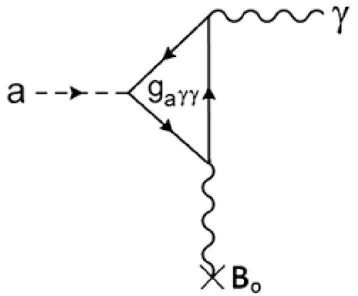

$$\mathcal{L}_{a\gamma\gamma} \propto g_{a\gamma} a \vec{E} \cdot \vec{B}_e$$

Haloscope: a resonant cavity immersed in a magnetic field for galactic dark matter axion conversion into microwave photons.

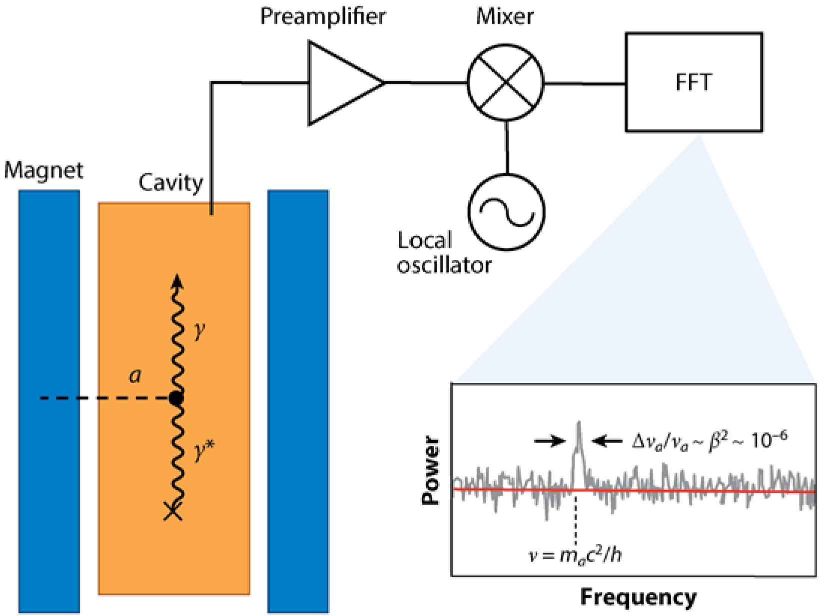

Haloscope experiments → ADMX, HAYSTAC, CAPP, QUAX, MADMAX, RADES, …

RADES colaboration

The team

KIT, Aalto U., MPP, Zaragoza U., CERN, Barcelona U., Cartagena U., LPENS, IFIC, ICMAB, IFAE, ITA, Bonn U., DESY, …

Expertise in:

- Cryogenics
- Cavities and MW filters
- Particle physics
- Quantum devices
- Magnetic materials
- …

ERC Synergy grant: DarkQuantum

Enhance haloscope searches with quantum techniques.

- **Low frequency range:** 200-500 MHz (1-2 μeV). Squid amplifiers (more info in J.M. García Barceló talk)
- **High frequency range:** 8-18 GHz (30-75 μeV). Quantum readout to surpass Standard Quantum Limit.

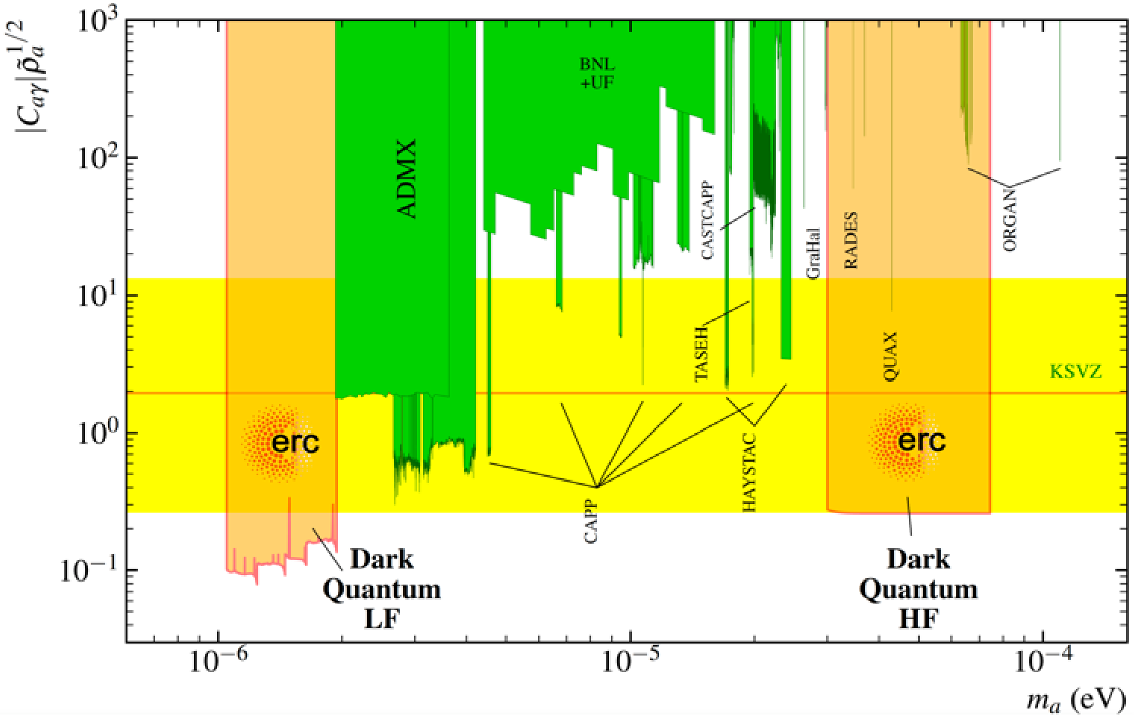

PI researchers:

- Igor G. Irastorza (Unizar, Zaragoza)
- Takis Kontos (LPENS, Paris)
- Sorin Paraoanu (Aalto University, Helsinki)
- Wolfgang Wernsdorfer (KIT, Karlsruhe)

Collaborators:

- MPP (Munich)
- Universidad Politécnica de Cartagena (Region de Murcia)
- DESY (Hamburg)
- Laboratorio subterráneo de Canfranc (Huesca)
- ICMAB (Barcelona)

Move from measuring IQ conjugate variables to Nϕ and measure only one of them

Measuring power

Axion conversion induces
a displacement in IQ plane

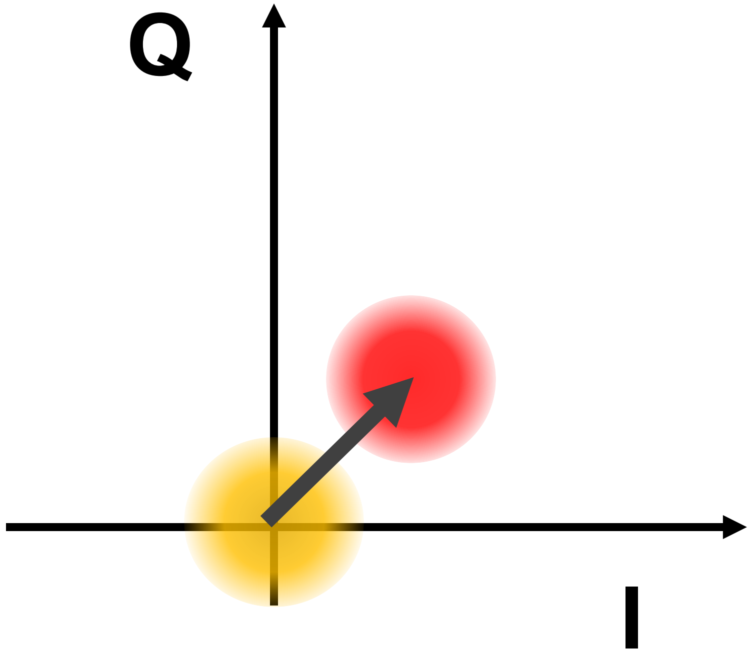

Move from measuring IQ conjugate variables to Nϕ and measure only one of them

Measuring power

Axion conversion induces a displacement in IQ plane.

Acual displacement could be tiny compared to noise.

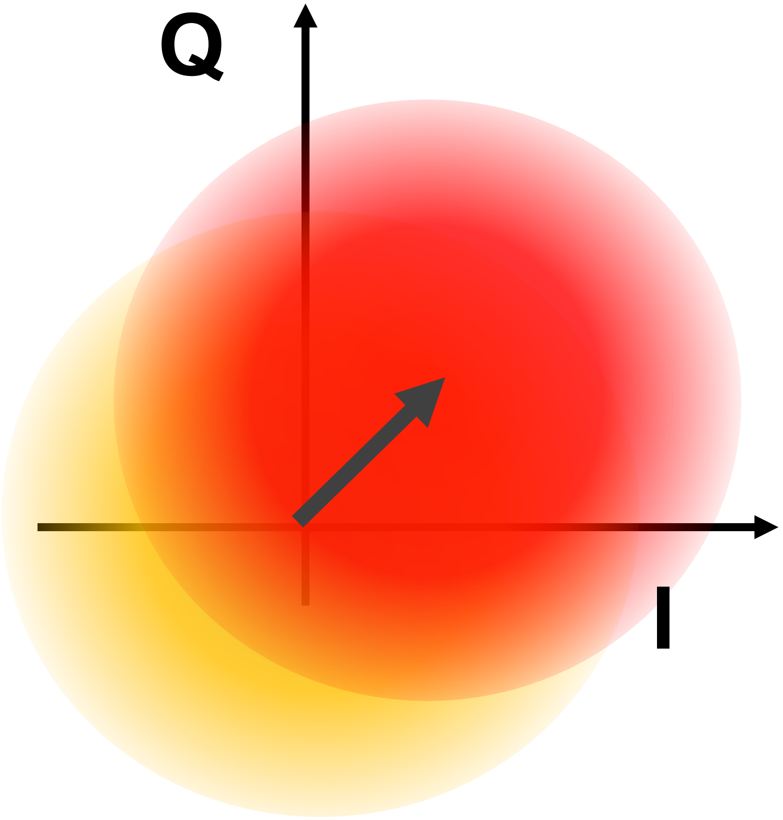

Quantum readout of an haloscope

Move from measuring IQ conjugate variables to Nϕ and measure only N

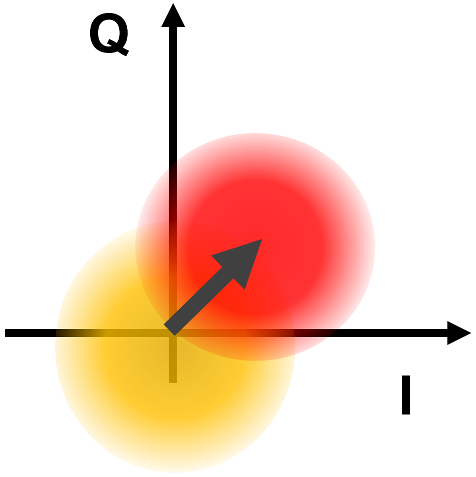

Measuring power (IQ)

Counting photons (N)

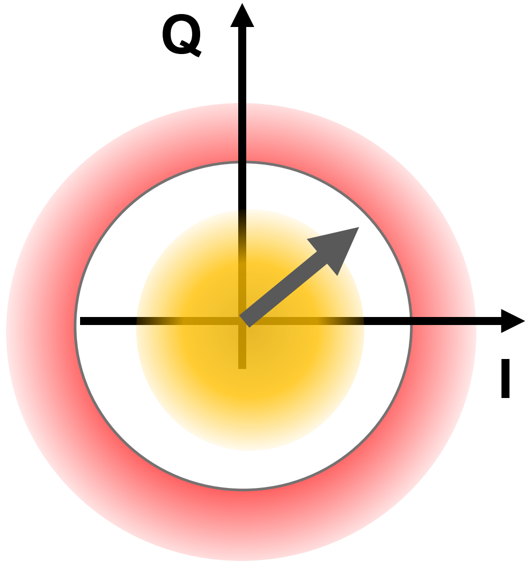

Measuring phase (ϕ)

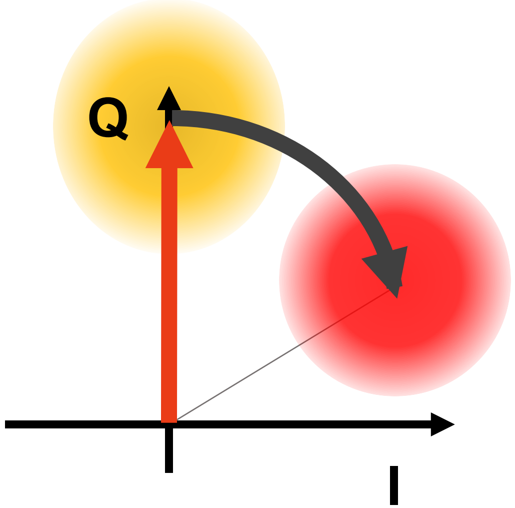

Quantum readout of an haloscope

Move from measuring IQ conjugate variables to Nϕ and measure only N

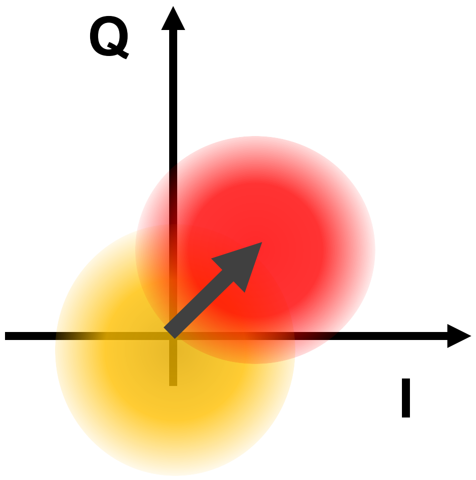

Measuring power

Counting photons

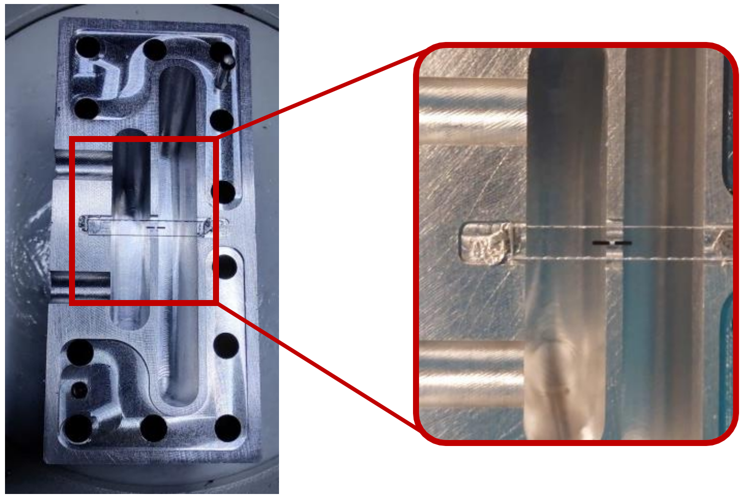

Microwave single photon counter

Measuring phase (ϕ)

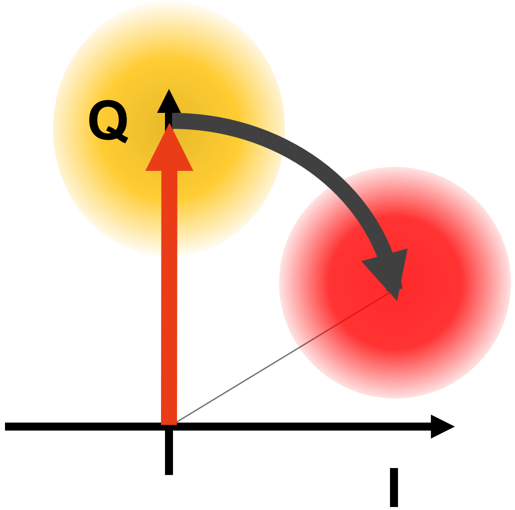

Quantum readout of an haloscope

Move from measuring IQ conjugate variables to Nϕ and measure only N

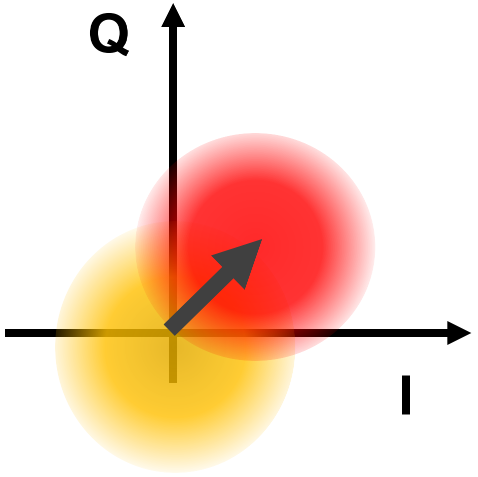

Measuring power

Counting photons

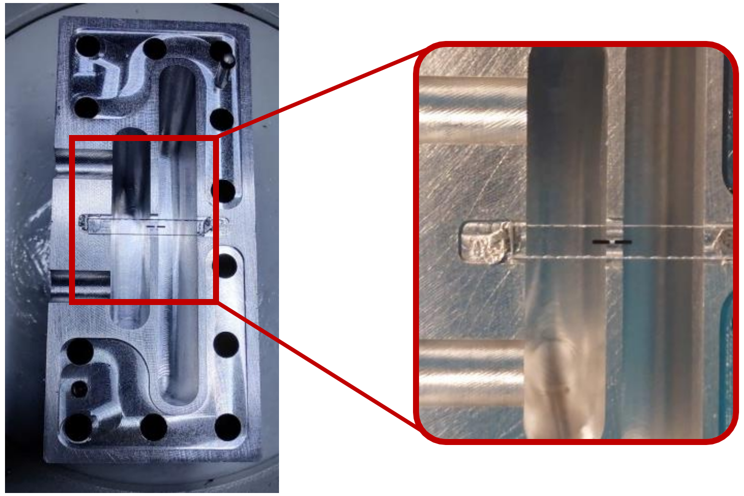

Microwave single photon counter

Measuring phase (ϕ)

Phase resolved haloscope

Overcome standard quantum noise limit

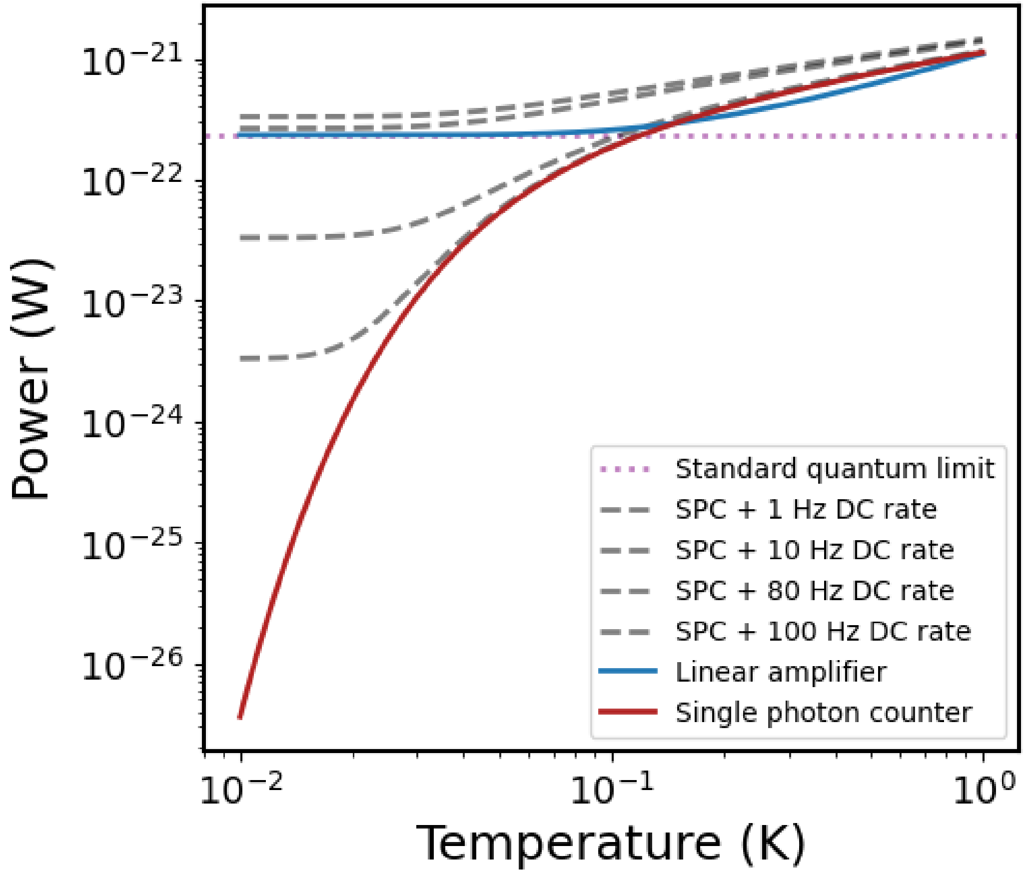

(f=5 GHz, Q=10^6, t=1s)

Linear receiver:

$$P_{LR} = h\nu(\bar{n}+1)\sqrt{\frac{\Delta\nu}{t}}$$

Standard quantum limit:

$$P_{SQL} = h\nu\sqrt{\frac{\Delta\nu}{t}}$$

Single photon counter (SPC)

$$P_{SPC} = h\nu_a\frac{\sqrt{N}}{t} = h\nu_a\sqrt{\frac{2\pi\nu\bar{n}}{Q_c t}}$$

Lamoreaux et al. Phys. Rev. D 88, 035020 (2013)

Working principle

- Readout cavity: To check the state of the transmon
- Transmon: Superconducting qubit
- Storage cavity: dark matter conversion into photons

Characteristic qubit frequency changes when a photon appears in the storage cavity.

Readout sequence designed to be sensitive to storage photon presence and to reduce quantum errors through quantum non-demolition measurements.

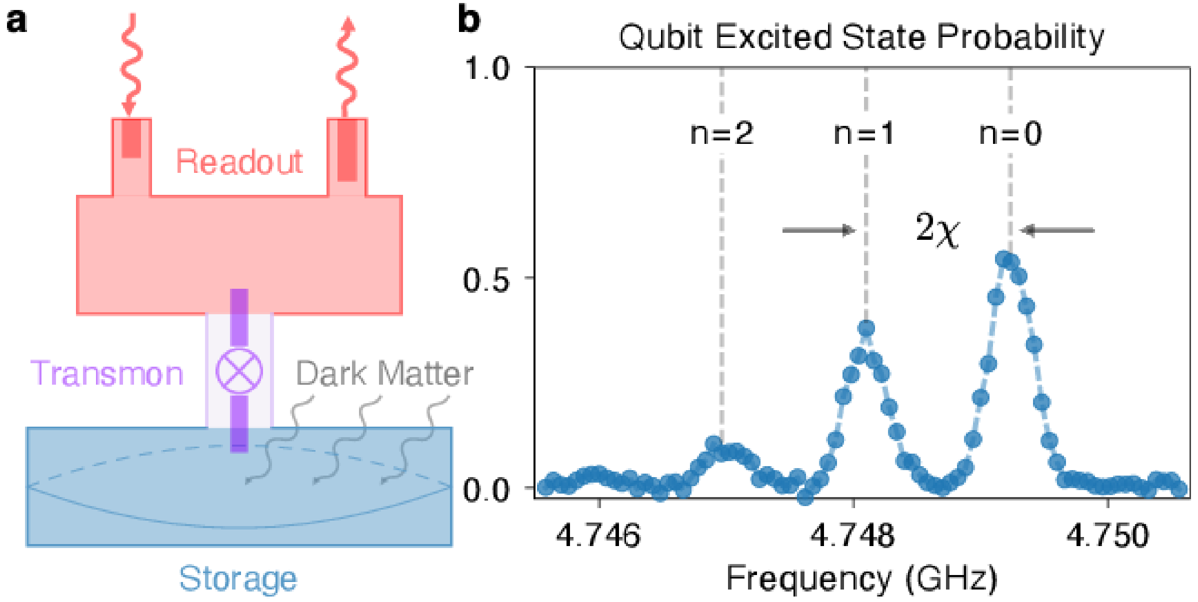

Dixit et al. Searching for dark matter with a superconducting qubit, Phys. Rev. Lett. 126

Ingredients for a microwave SPC

Double cavity
(Readout + Storage)

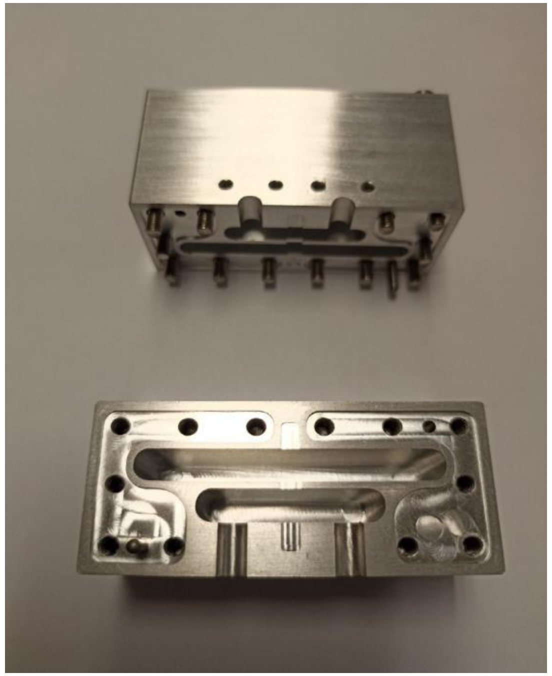

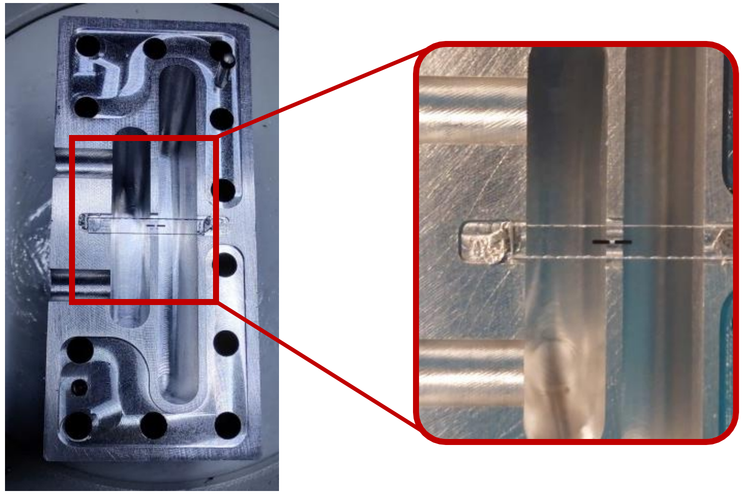

Cold!

Dilution refrigerator: 10-20 mK

Transmon

(Optical microscope)

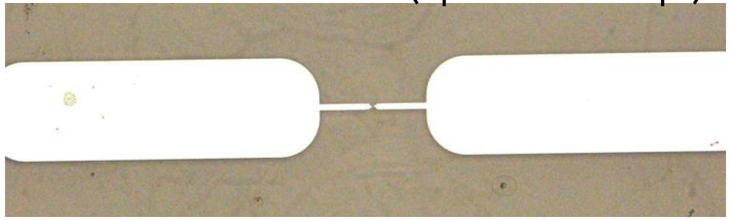

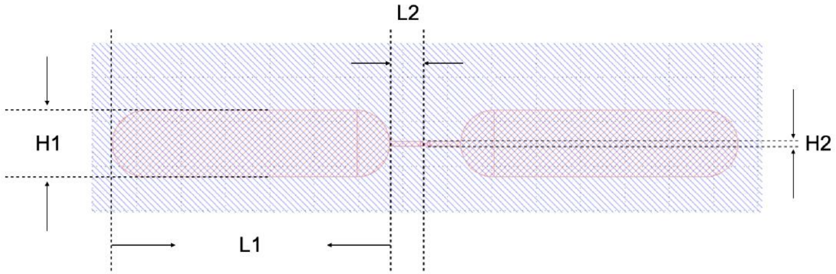

	Q1
L1 (mm)	1
H1 (mm)	0.3
L2 (mm)	0.15
H2 (mm)	0.02

Parity measurement

Interferometric measurement.

Precession of qubit state in the Bloch sphere dependent on photon content.

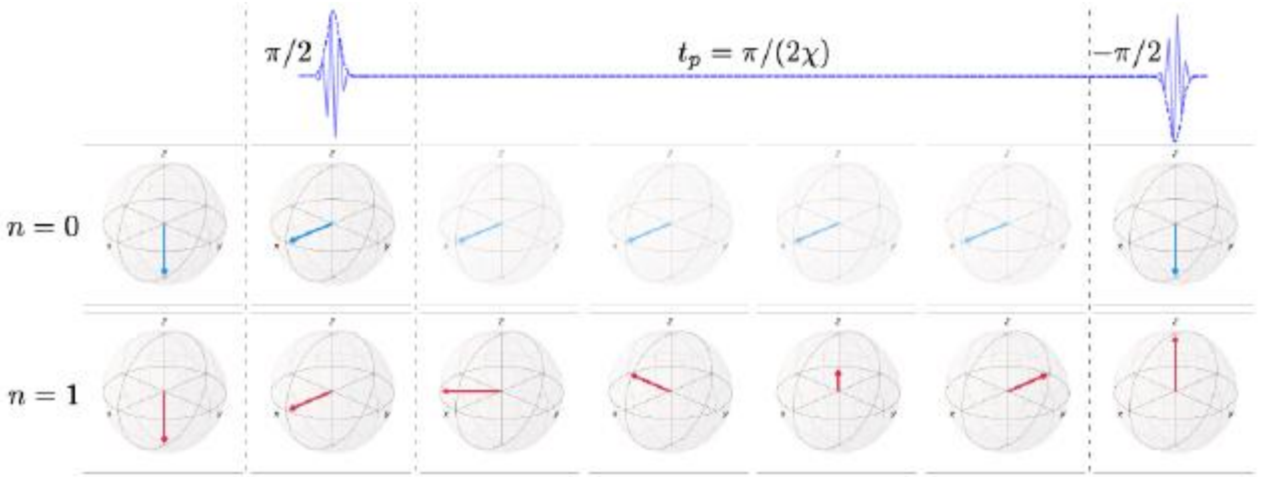

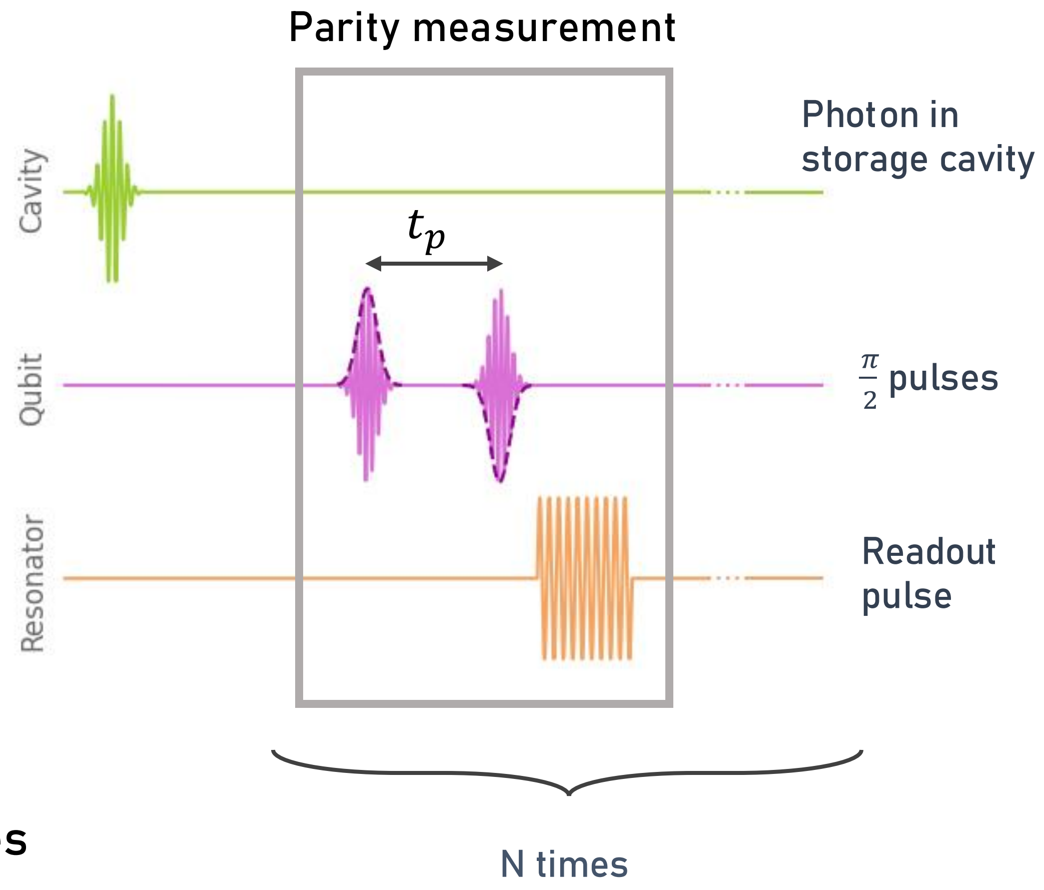

Parity sequence: ($\pi/2$ + Wait t_p + $-\pi/2$ + Readout) x N times

Parity sequence

Injecting photons

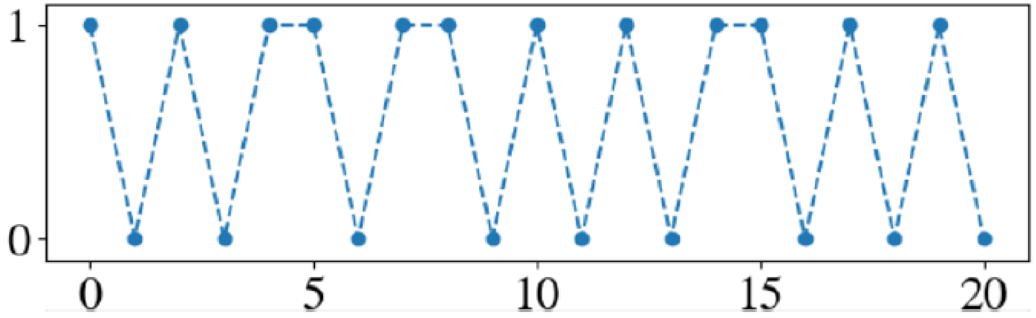

Not injecting photons

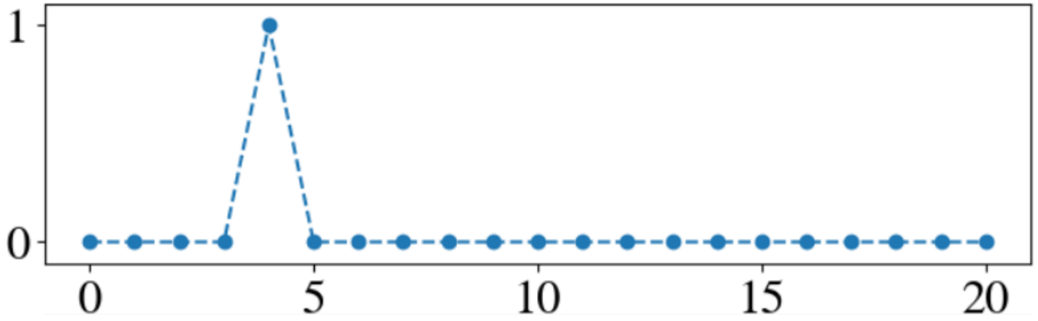

N = 21

Nth measurement

Nth measurement

Probabilities of hidden states: Hidden Markov Model

Photon in storage cavity

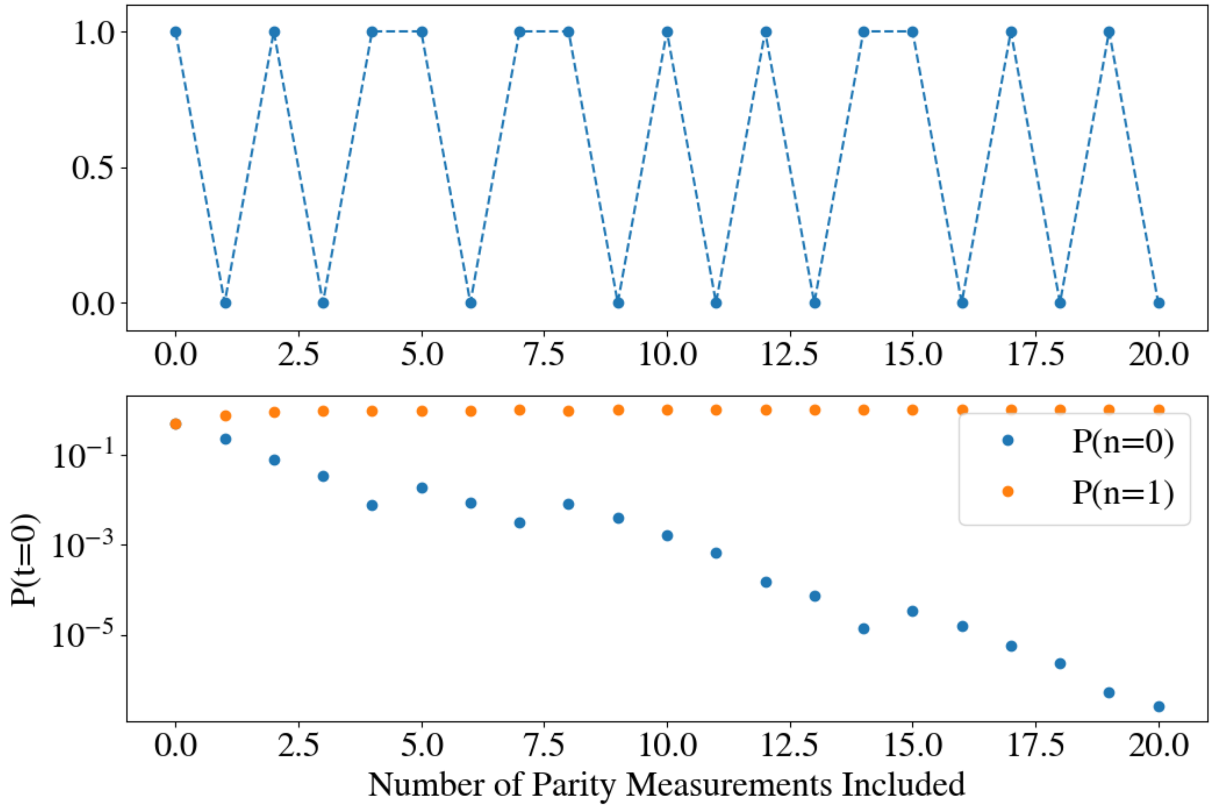

No photon in storage cavity

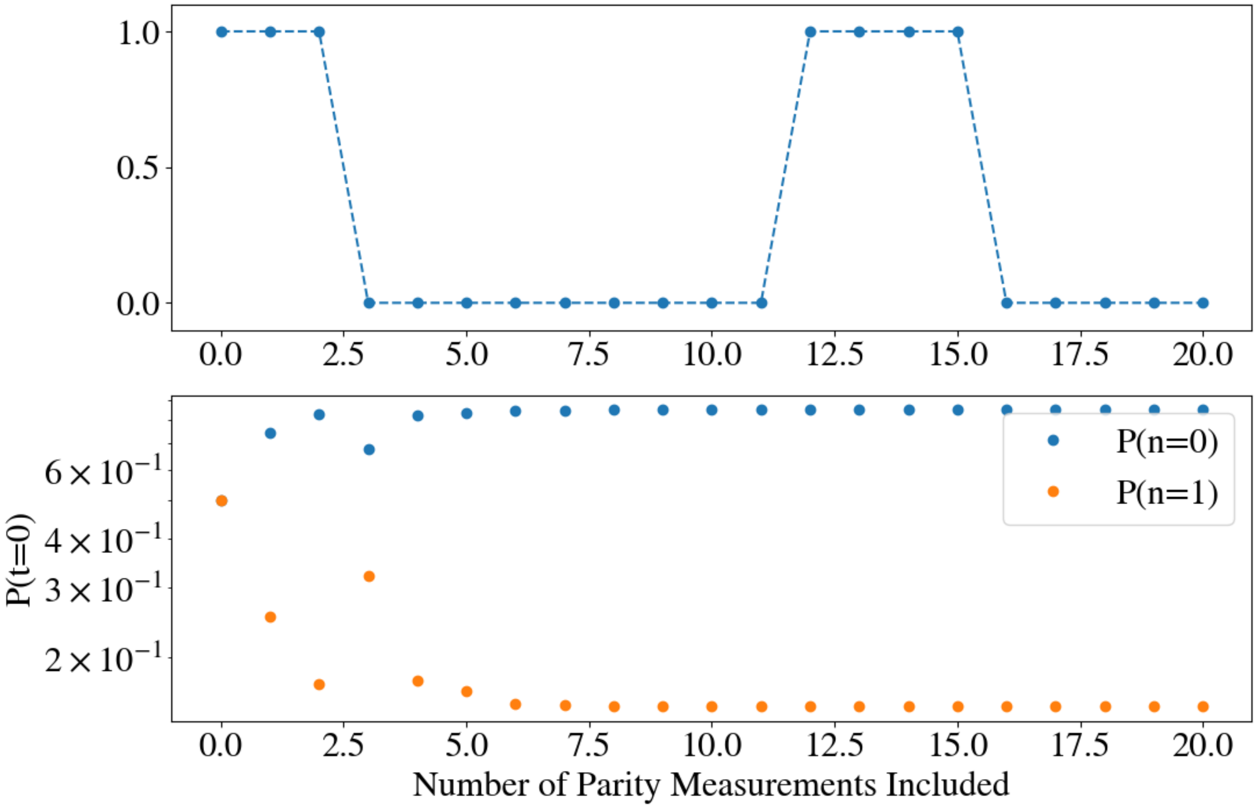

Non demolition measurement

Distributions of likelihood test

Likelihood test: $\lambda = \dfrac{P(n_0 = 1)}{P(n_0 = 0)}$

Calibrations

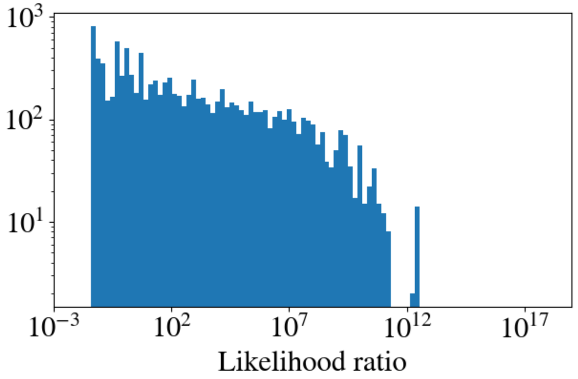

Injecting photons in the storage cavity

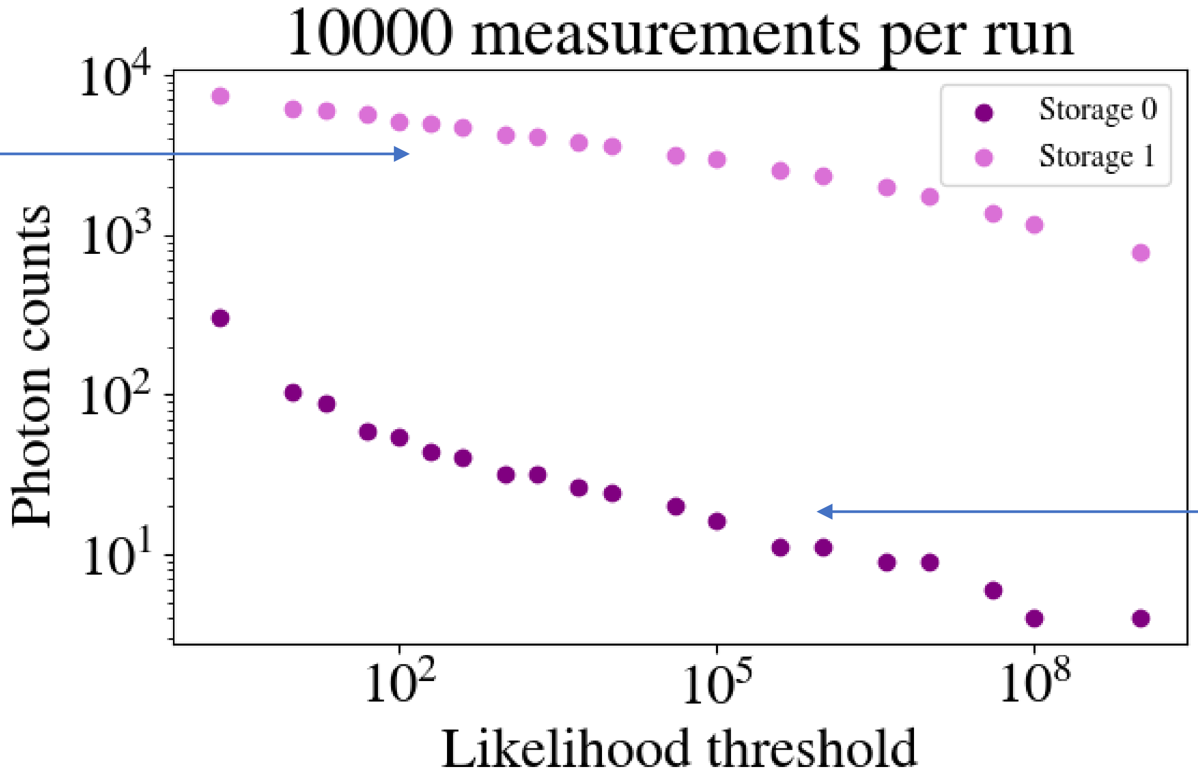

Background

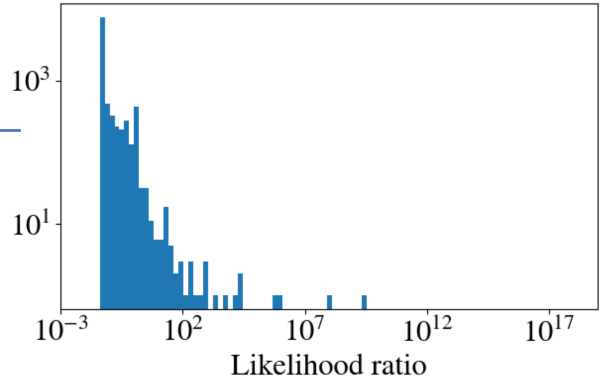

Likelihood threshold: Chosen λ value to discriminate the presence of a photon.

First RADES runs in Aalto University

	$\Pi/2$	t_p	$-\Pi/2$	Readout	Delay	t_m	Total time (N=21)
Run 1	52 ns	88 ns	52 ns	800 ns	100 ns	1092 ns	22.932 us
Run 2	52 ns	88 ns	52 ns	800 ns	100 ns	1092 ns	22.932 us

Two runs with 10000 parity sequences each.
Same parameters in both runs.

Background rate estimation

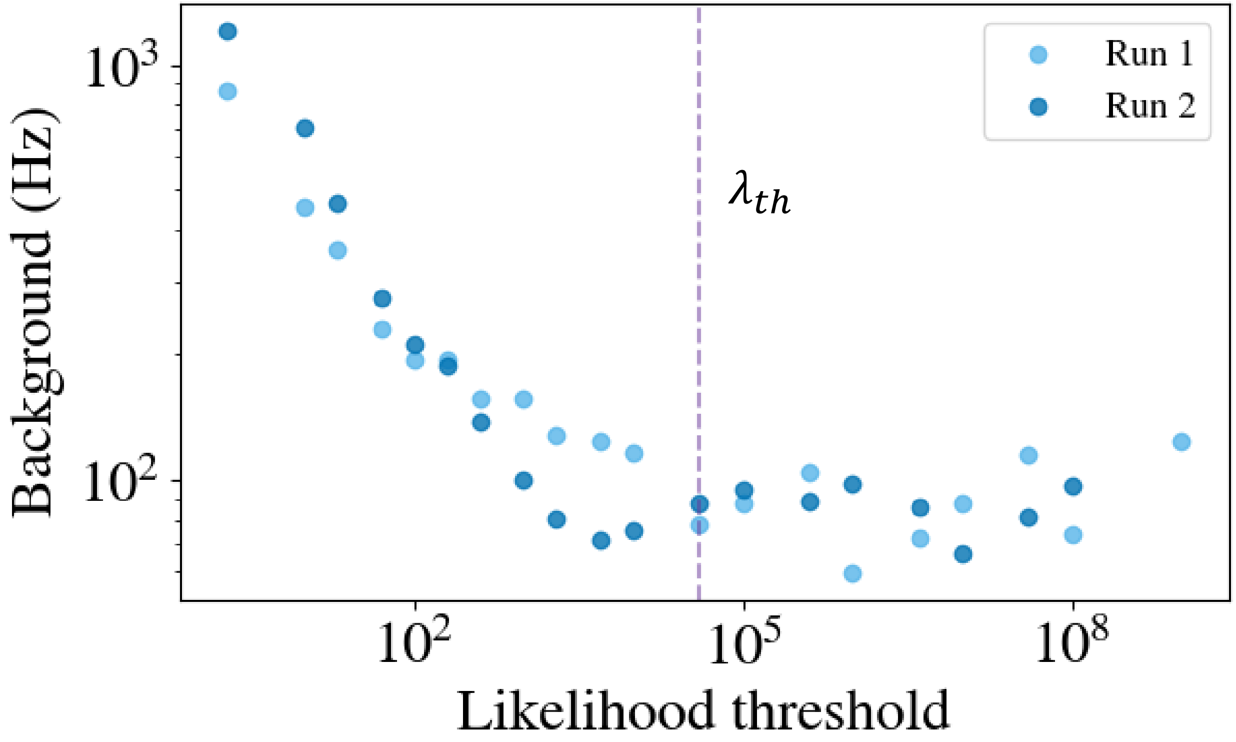

10000 measurements
$T_1^s = 20\ \mu s$
$\lambda_{th} = 4 \times 10^4$

$\lambda_{th} = 4 \times 10^4$	Background (Hz)	Efficiency	Live time (s)
Run 1	77.94	25.7%	0.2
Run 2	87.35	28.6%	0.2

Exclusion limits

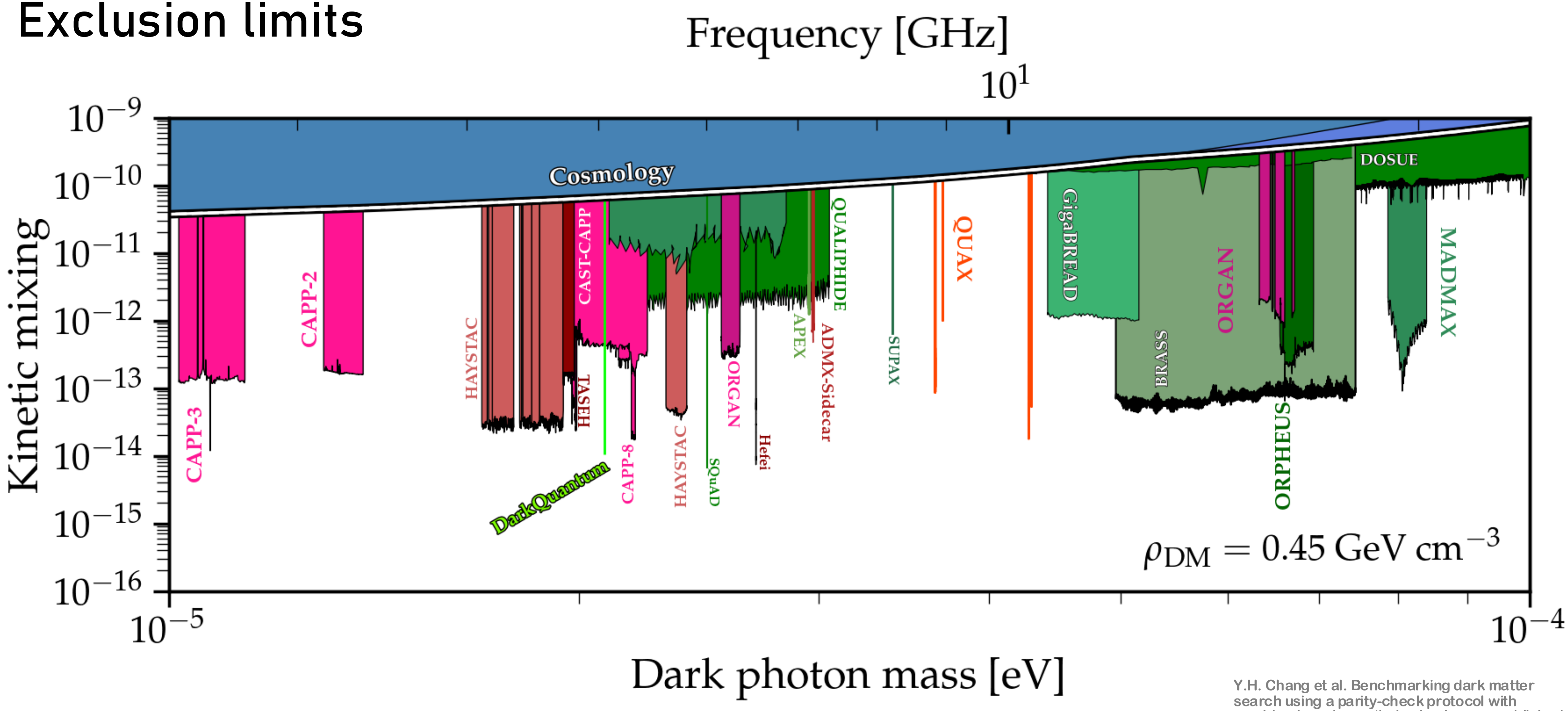

Y.H. Chang et al. Benchmarking dark matter search using a parity-check protocol with machine-learning optimized pulses, unpublished.

Scale up

- Increase volume for higher sensitivity
- Test mode clustering and qubit couplings

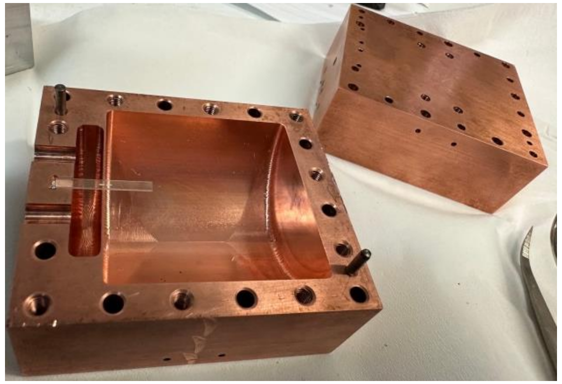

Tuning sytems

- Vertical cut tunning
- Ferromagnetic tuning (YIG)

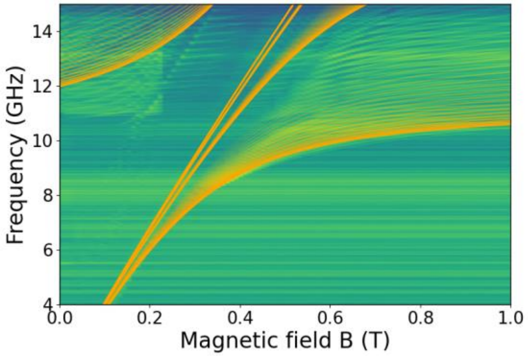

Magnetic field

- Magnetic resilient qubits: Granular aluminium
- Shielding and counter coils

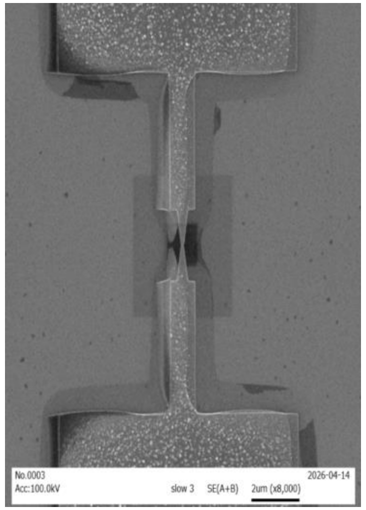

Phase resolved haloscope

Look for a coherent signal interfering with a known reference tone.

Coherent axion signal with coherence time dependent on the linewidth:

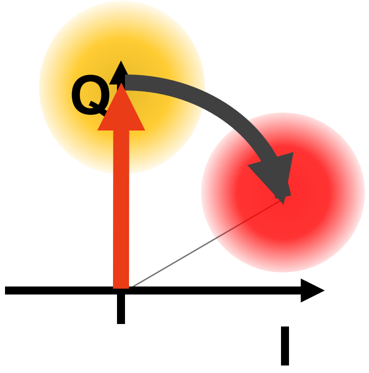

$$\tau_a = \frac{Q_a}{f} \Rightarrow 5GHz\ axion\ \rightarrow \tau_a = \frac{10^6}{5 * 10^9 Hz} = 200\ \mu s$$

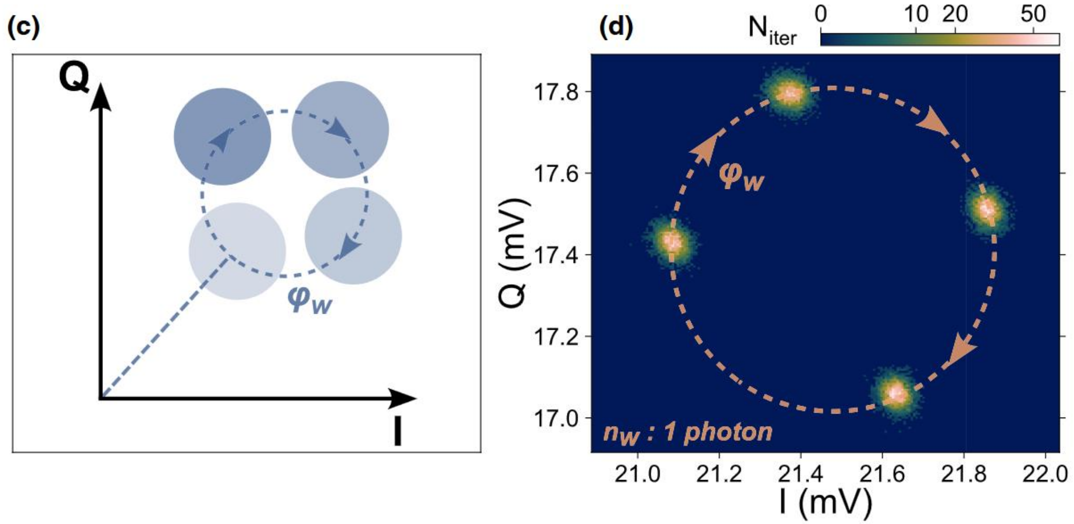

Axion phase measured with respect a coherent reference tone (â)

$$\Delta\omega_q = K\ [\ |\hat{a}|^2 + |\hat{a}_{ax}|^2 + 2|\hat{a}||\hat{a}_{ax}|\cos(\varphi_{ax})]$$

The random phase of the axion signal makes the state rotate in IQ plane due to interference pattern.

Diameter of the rotation proportional to the axion signal amplitude.

Phase resolved haloscope

Pulse sequence:
- Continous refence tone at detection mode (yellow).
- Ramsey interferometry pulses (green).
- Readout tone (red).

Axion weak tone injected for calibration (blue).
Amplitude and phase of the weak tone vary.

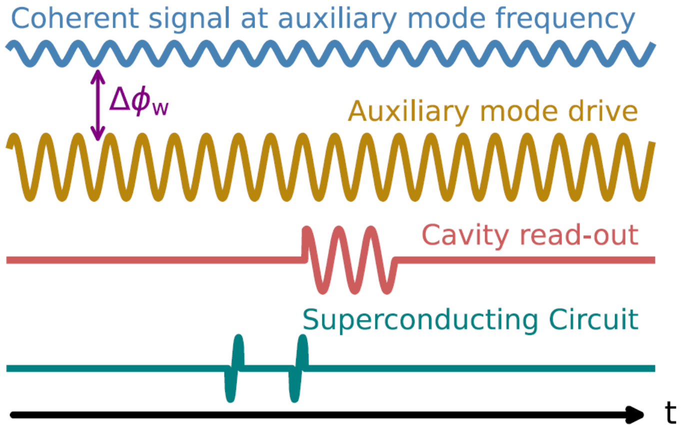

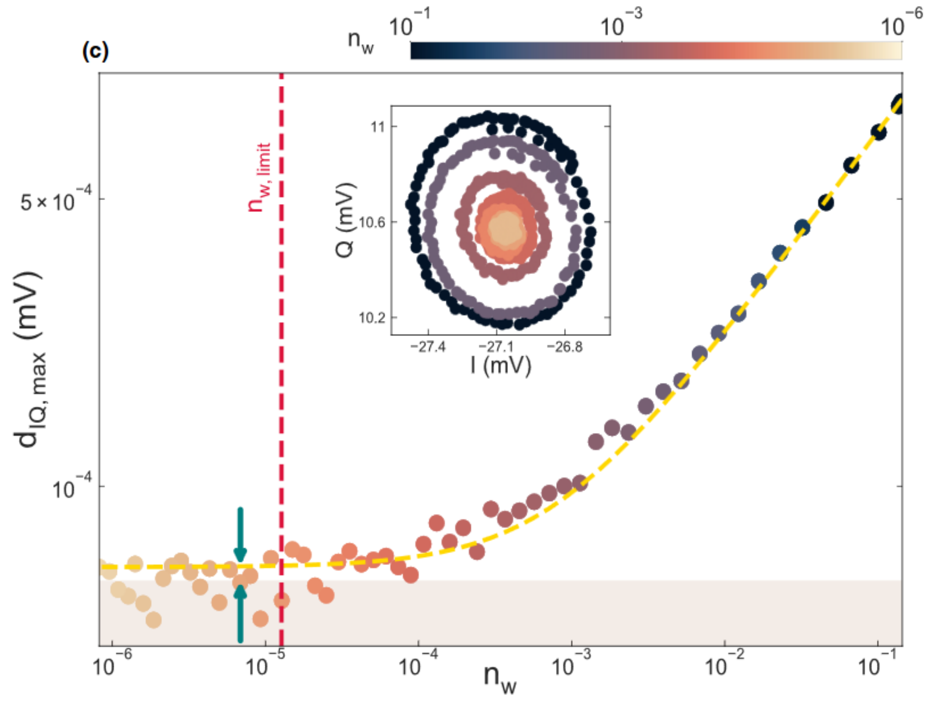

Varying pahse: circles in IQ plane
Varying amplitude: diameter of the circles
Smallest detectable signal: circles become a blob

Granular aluminium transmons

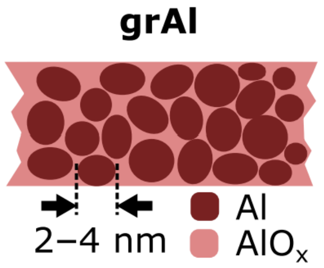

Transmon: Granular aluminium with niobium pads.
Weak anharmonicity K = 200 ± 50 kHz
This has disadvantages but helps in a high density photon environment (pump).
Works ongoing to increase anharmonicity

Al grains in a AlO matrix.

Behaves like a chain of Josephson junctions.

Superconducting circuit consisting in two pads and a point-contact union.

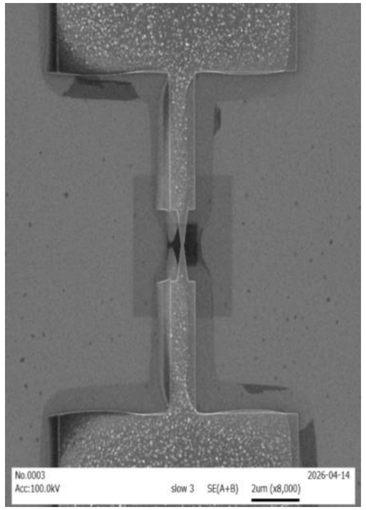

Rabi oscillations with in-plane B field

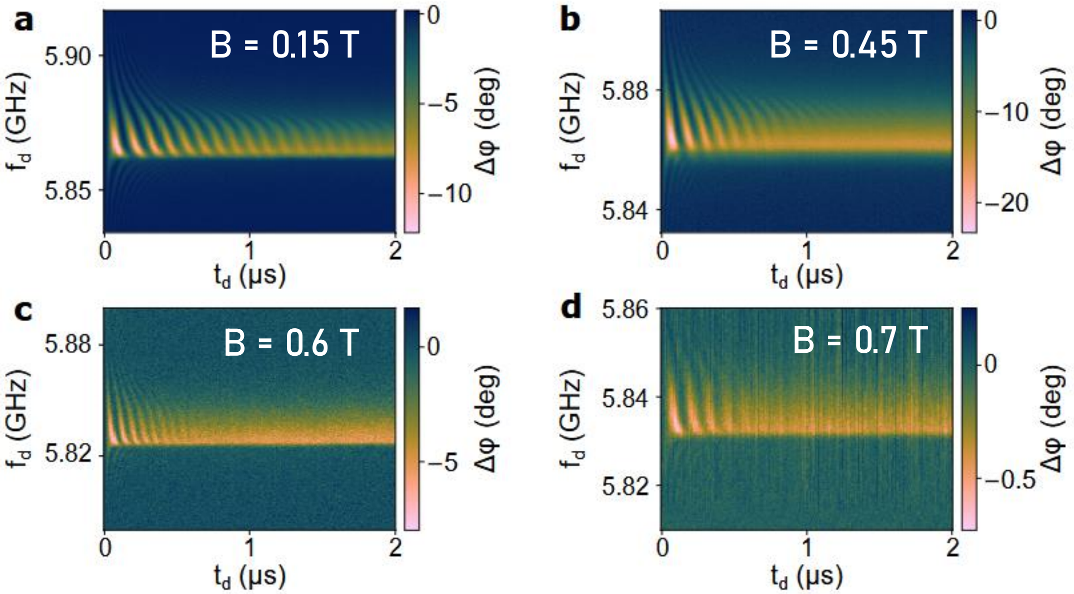

Magnetic tuning

YIG cylinder: 1 cm long, 5mm diameter
Resonant frequencies dependent on B field applied.
Ongoing work: Identification of axion mode and from factor characterization

Experimental measurement

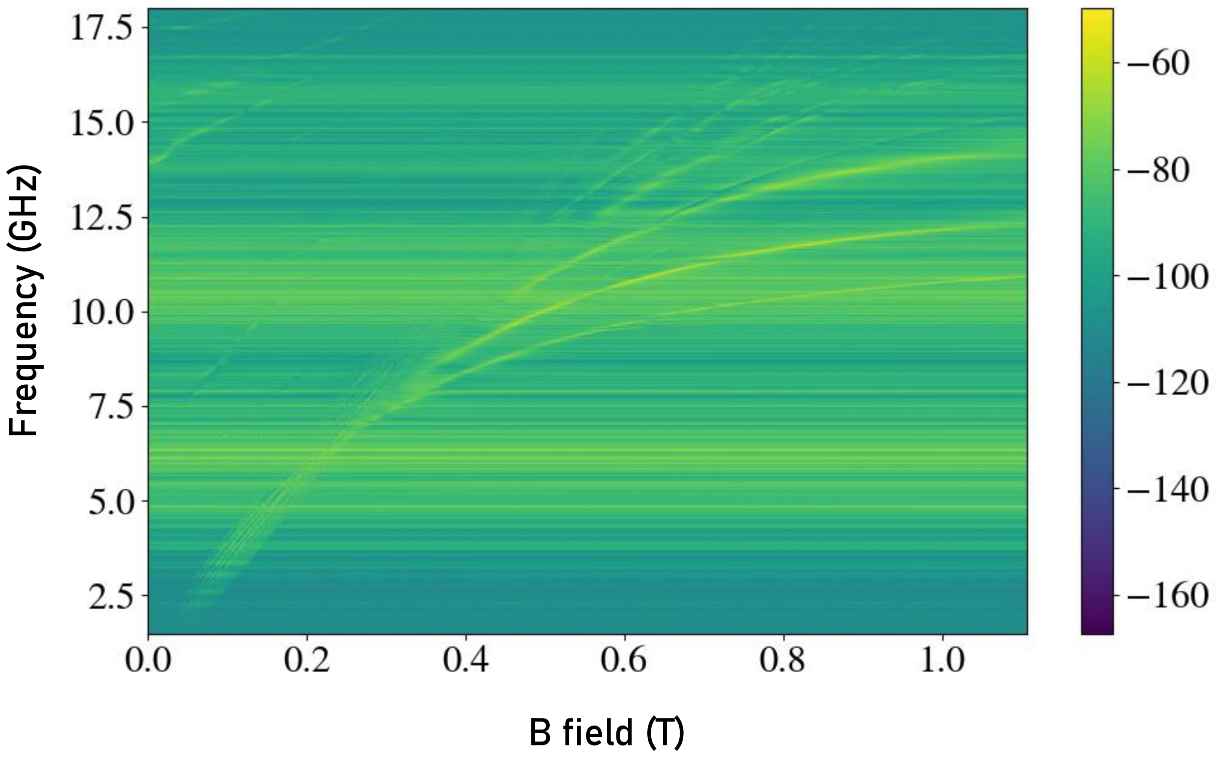

Comsol simulation

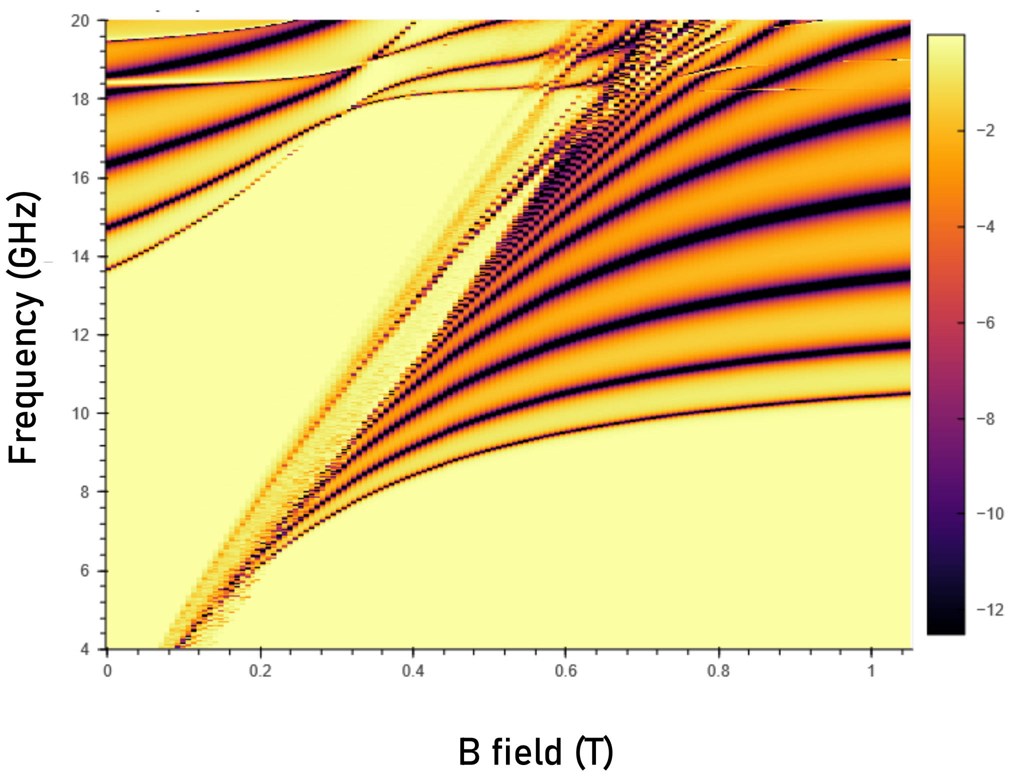

Sensitivity prospects

If both branches of YIG resonances can be followed and assuming reachable sensitivity during data takings as in the first calibration these are the sensitivity prospects for axion searches:

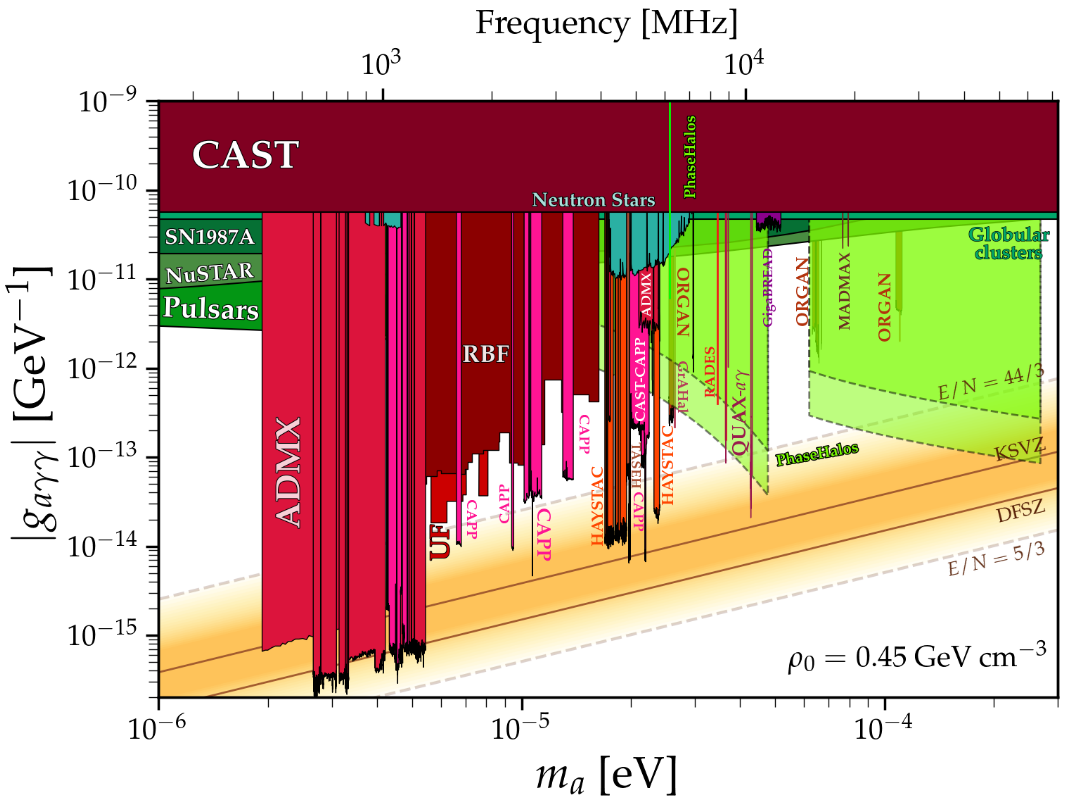

For 90% C.L. → SNR = 1.28

$$SNR = \frac{P_{sig}}{\sigma_{noise}} = \frac{P_{sig}}{S_P}\sqrt{t}$$

Axion prospects:

$$P_{sig} = g^2 \frac{\rho}{m_a} B^2 V G Q \frac{\beta}{1+\beta}$$

Parameter	Value
S_P	$1.2 \cdot 10^{-22(23)}\ W/\sqrt{Hz}$
Integration time (t)	10^3 s
V	$30\ cm^3$
Q	10^5
B	0-2 T
G	0.5
β	2

Next steps phase haloscope

Improve GrAl circuits

- Calibrating evaporator for higher accuracy in oxygen pressure and growing rate.
- Increase anharmonicity

Background runs w/o B field

- Improve pulse sequence for background run.
- Data managing in longer runs.
- Test other qubits with the same protocol.

Phase jamming calibration

- Develop a 1 kHz source
- Phase shifts randomly
- Mimic axion signals better than any other calibration source.

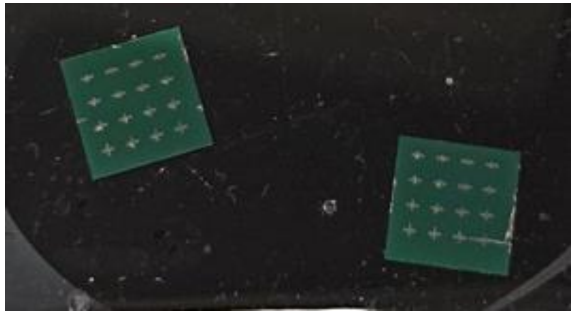

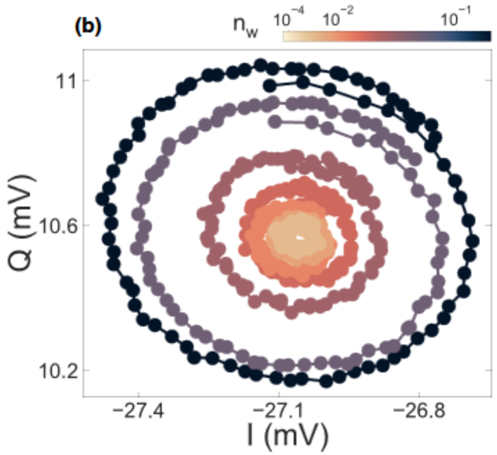

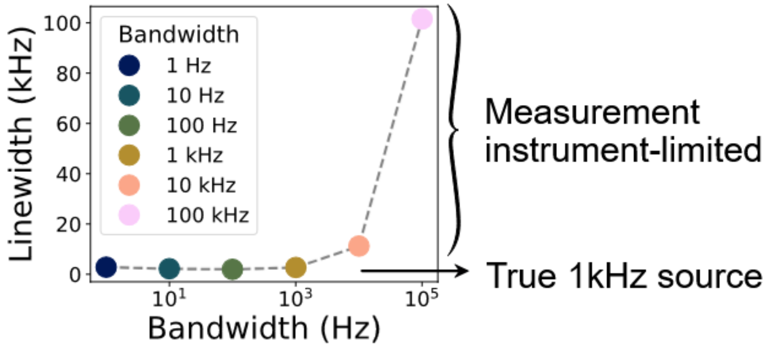

Quantum haloscopes in RADES

- Range of interest: 8-18 GHz (30-75 µeV)
- First prototype: microwave single photon counter with aluminum transmon.
- Biggest challenge: superconducting circuits in magnetic field.
- Granular aluminum devices may be able to operate at modest B fields.
- Two parallel strategies: Measure photon number or phase of the signal in order to surpass Standard Quantum Limit.
- Preparing setups with tuning systems to measure this year.

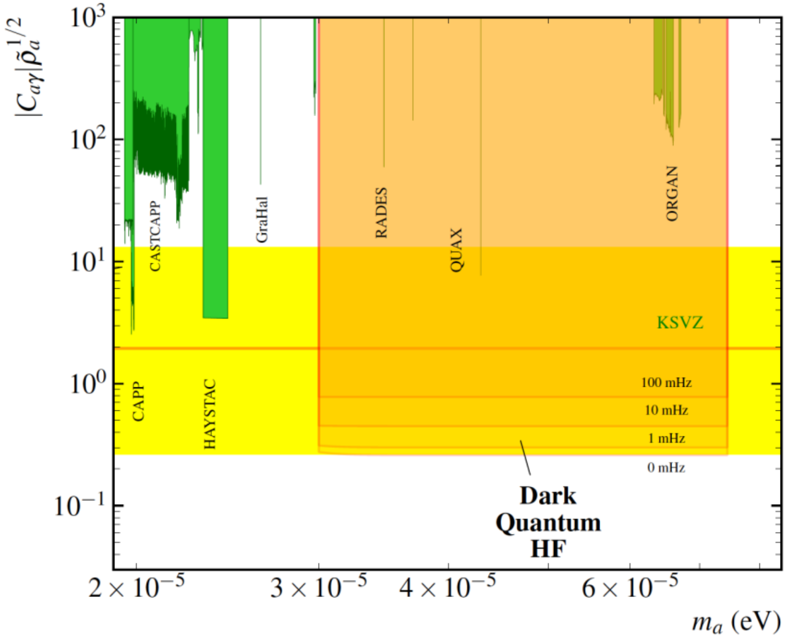

THANK YOU !!!

Back-up slides

Post-inflation QCD axion predictions

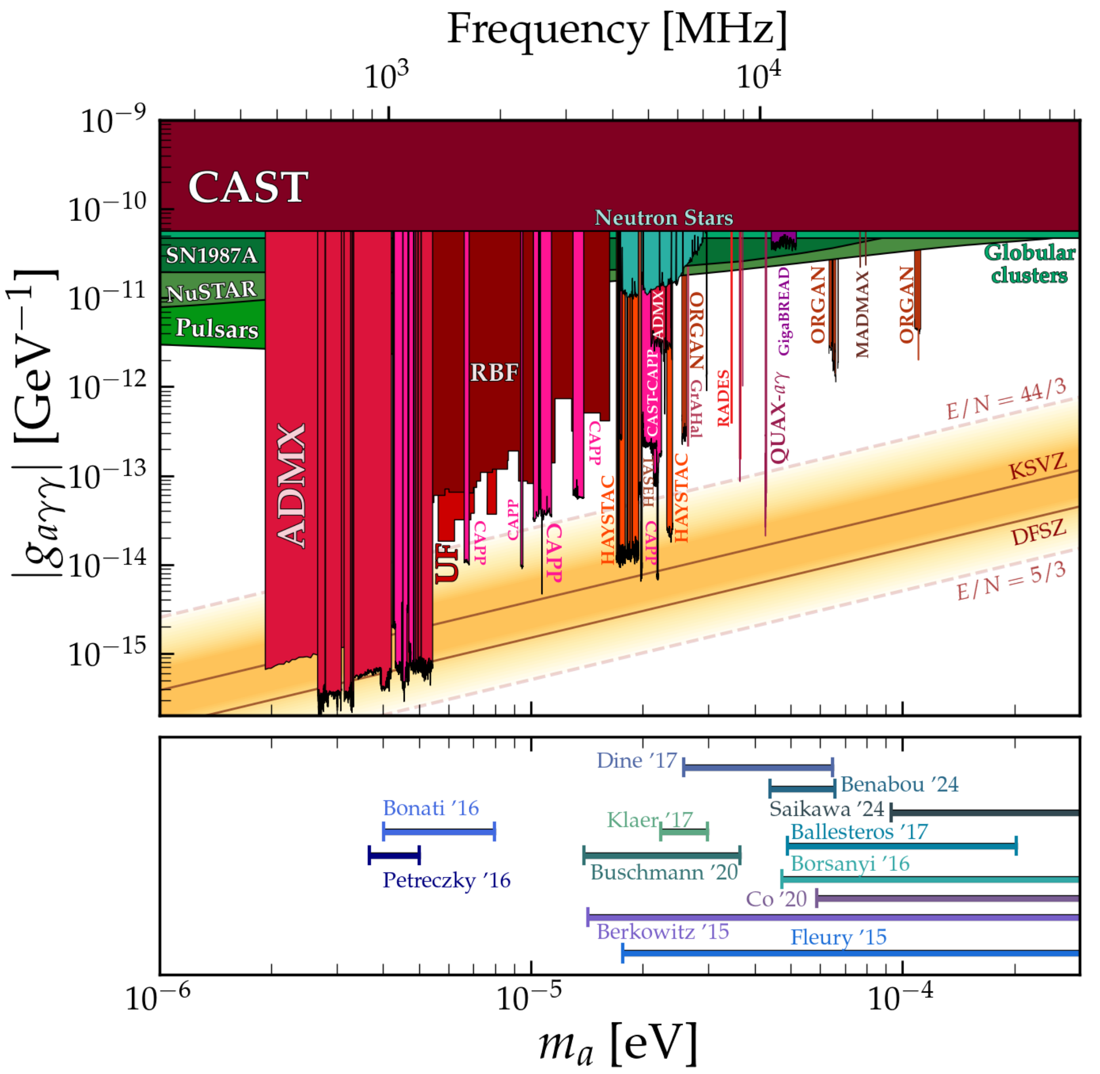

Double cavity

Frequencies

	Readout (f_r)	Storage (f_s)
Simulated	6.869 GHz	5.024 GHz
Measured	6.867 GHz	5.051 GHz

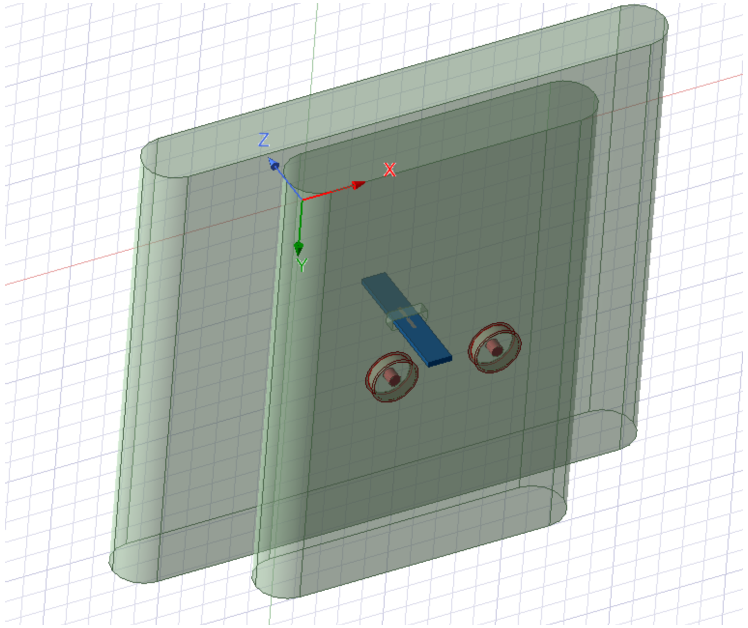

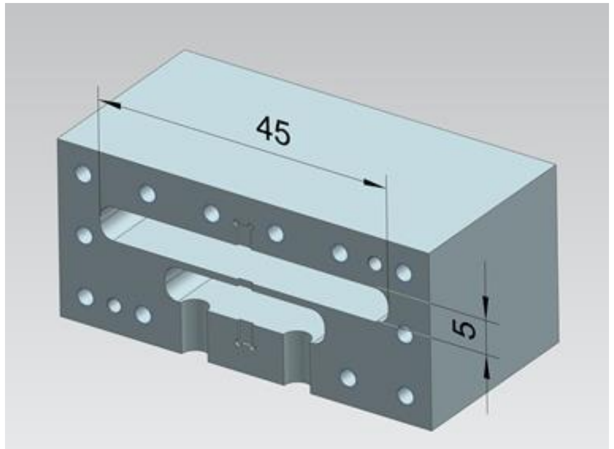

Aluminum

Copper

EM simulation: Ansys-HFSS
Qubit simulation: Black-box superconducting circuit quantization

S. Nigg et al. Black-box superconducting circuit quantization (2012)

Transmon: superconducting qubit

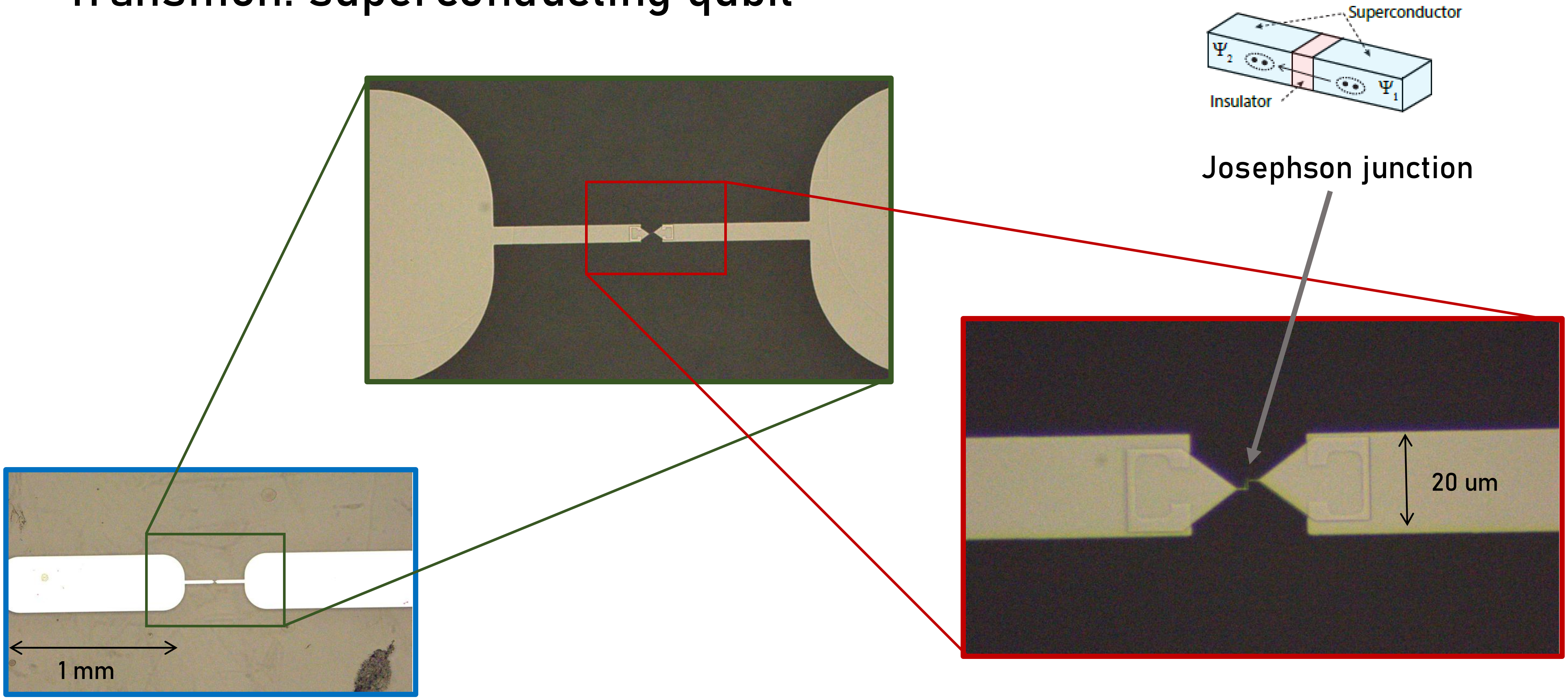

Bloch sphere

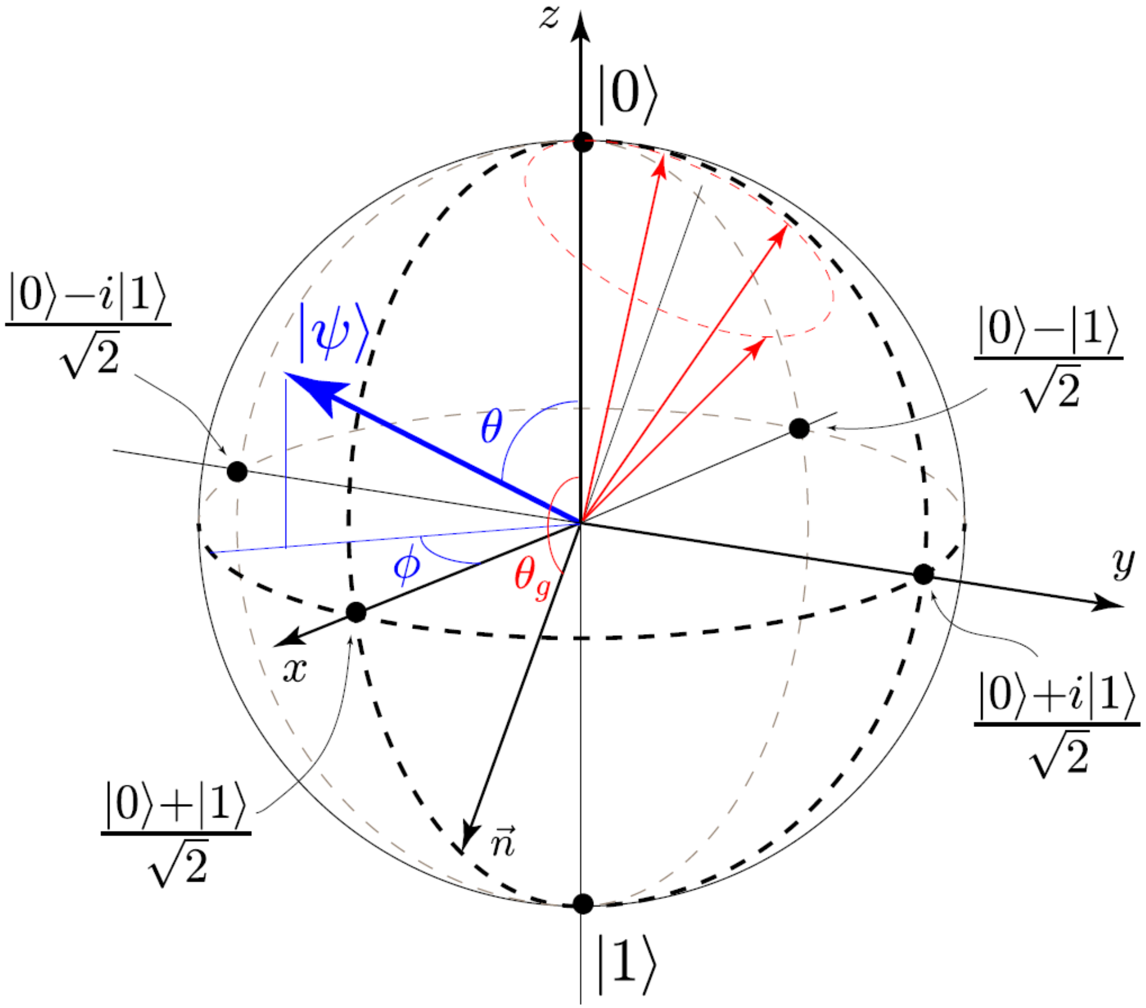

Readout fidelity

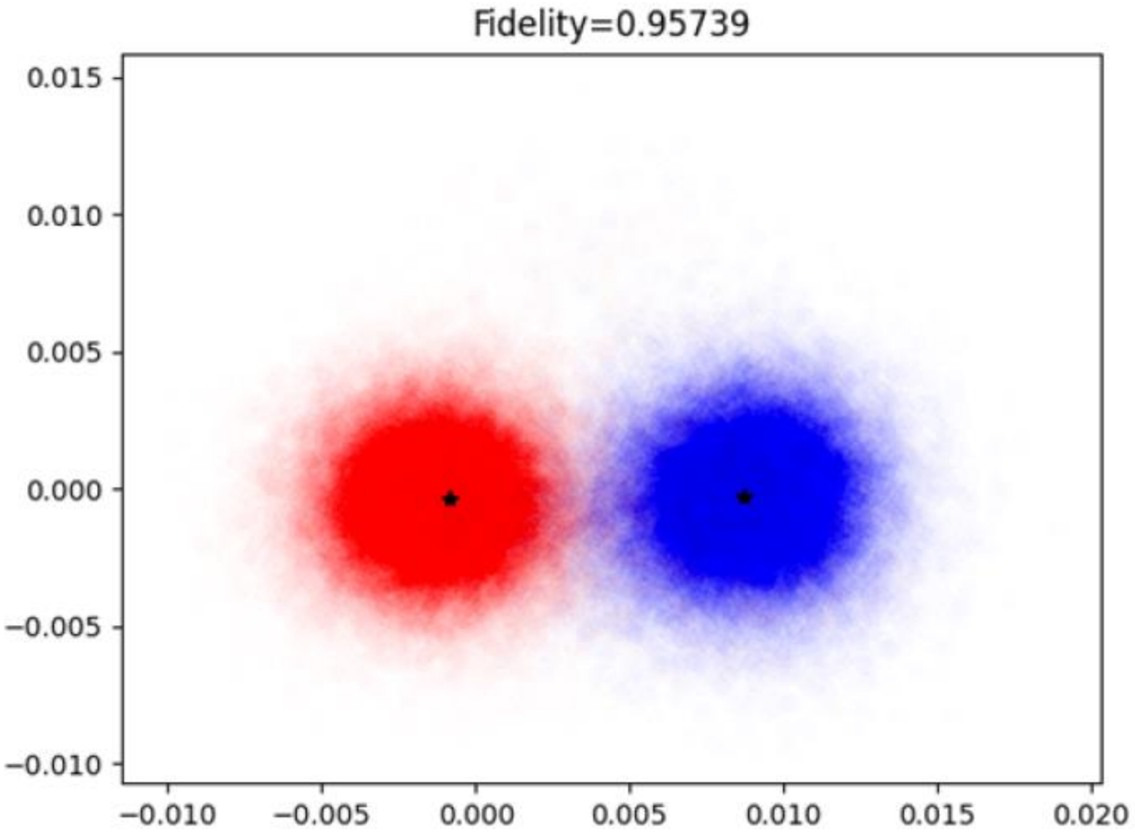

Figure 8: Readout fidelities. Blue measurements with qubit in ground state, red with qubit in first excited state.

- Prepare state
- Readout pulse
- Plot in IQ plane
- Set threshold value

Pairs of conjugate variables

[I,Q]=i [N,ϕ]=i

$$I = \frac{a + a^\dagger}{2} \qquad N = a^\dagger a$$

$$Q = \frac{a - a^\dagger}{2i} \qquad e^{i\phi} = (N+1)^{-1/2} a$$

$$N = a^\dagger a = I^2 + Q^2 - \frac{1}{2}$$

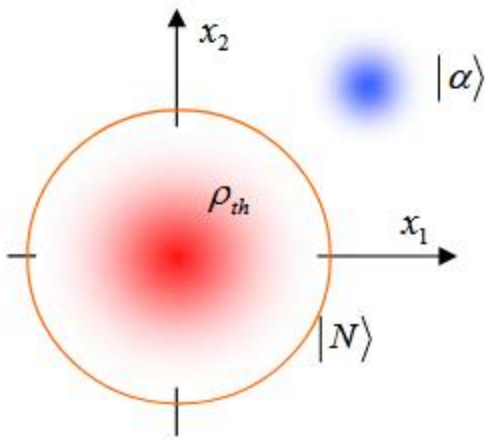

Coherent state in blue
Thermal state in red
Fock state in orange

- **Coherent state**: well-defined phase, Poissonian number distribution.
- **Fock state**: perfectly defined number → complete phase uncertainty.

Power measurement

$$P = \hbar\omega\langle a^\dagger a\rangle = \hbar\omega\langle N\rangle$$

$$\boxed{P = \hbar\omega\left(\langle I^2\rangle + \langle Q^2\rangle - \frac{1}{2}\right)}$$

Parameters of the single photon counter

Device parameter	Symbol	Value
Transmon frequency $\|g\rangle \longrightarrow \|e\rangle$	w_q	$2\pi \times 4.629$ GHz
Transmon frequency $\|e\rangle \longrightarrow \|f\rangle$	w_{ef}	$2\pi \times 4.357$ GHz
Sideband qubit-storage frequency $\|f0\rangle \longrightarrow \|g1\rangle$	w_{f0-g1}	$2\pi \times 3.935$ GHz
Transmon anharmonicity	α_q	$-2\pi \times 272$ MHz
Transmon decay time	T_1^q	16.7 μs
Transmon decoherence time	T_2^q	6.2 μs
Transmon background photon	$\bar{n}_q$	
Storage frequency	w_s	$2\pi \times 5.051$ GHz
Storage decay time	T_1^s	20 μs
Storage decoherence time	T_2^s	
Storage-Transmon Stark shift	2χ	$-2\pi \times 4.6$ MHz
Storage background photon	$\bar{n}_s$	
Readout frequency	w_r	$2\pi \times 6.867$ GHz
Readout-Transmon Stark shift	$2\chi_{qr}$	
Readout fidelity $\|g\rangle$	$F_{g\mathcal{G}}$	0.95739
Readout fidelity $\|e\rangle$	$F_{e\mathcal{E}}$	
Readout time	t_r	800 ns
Parity time	t_p	88 ns
90º rotation pulse time	$\pi/2$	52 ns
Waiting time between measurements	t_w	100/1000 ns
Time between parity sequences	t_t	1 ms

Table 3: Parameters of the single photon counter.

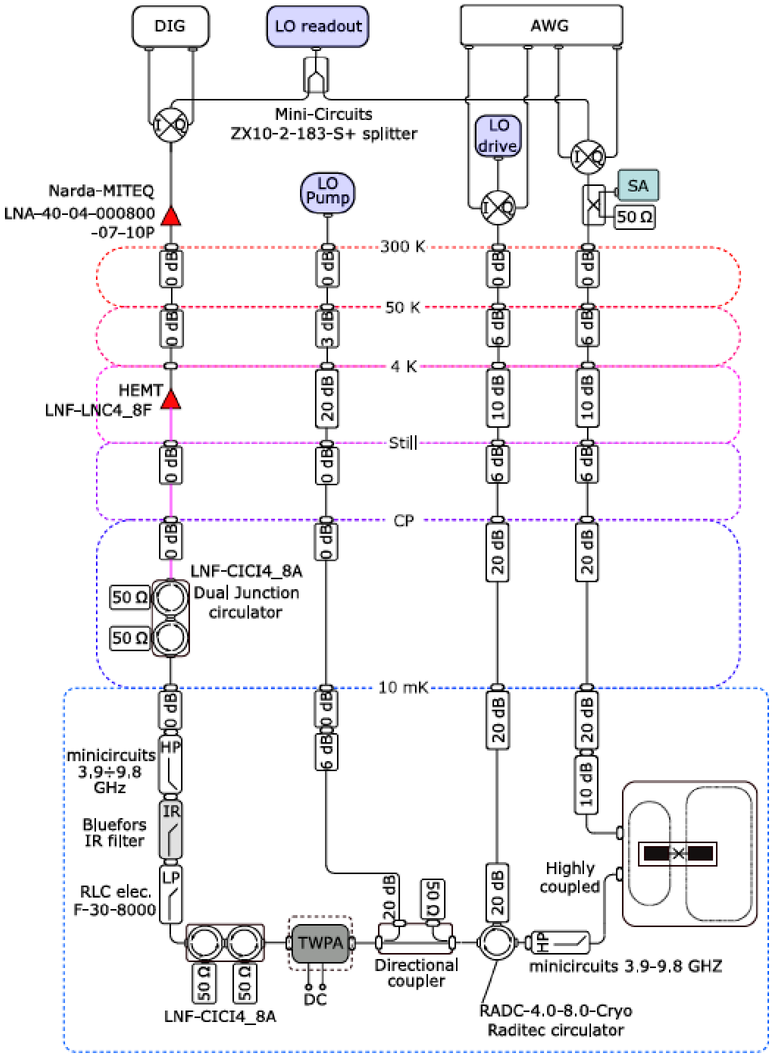

Figure 7.20: Layout of the input and output RF lines inside the cryostat during the parity measurements.

Bluefors LD dilution cryostat at MPP Munich

12 T magnet
Diameter: 7cm
Height: 40 cm

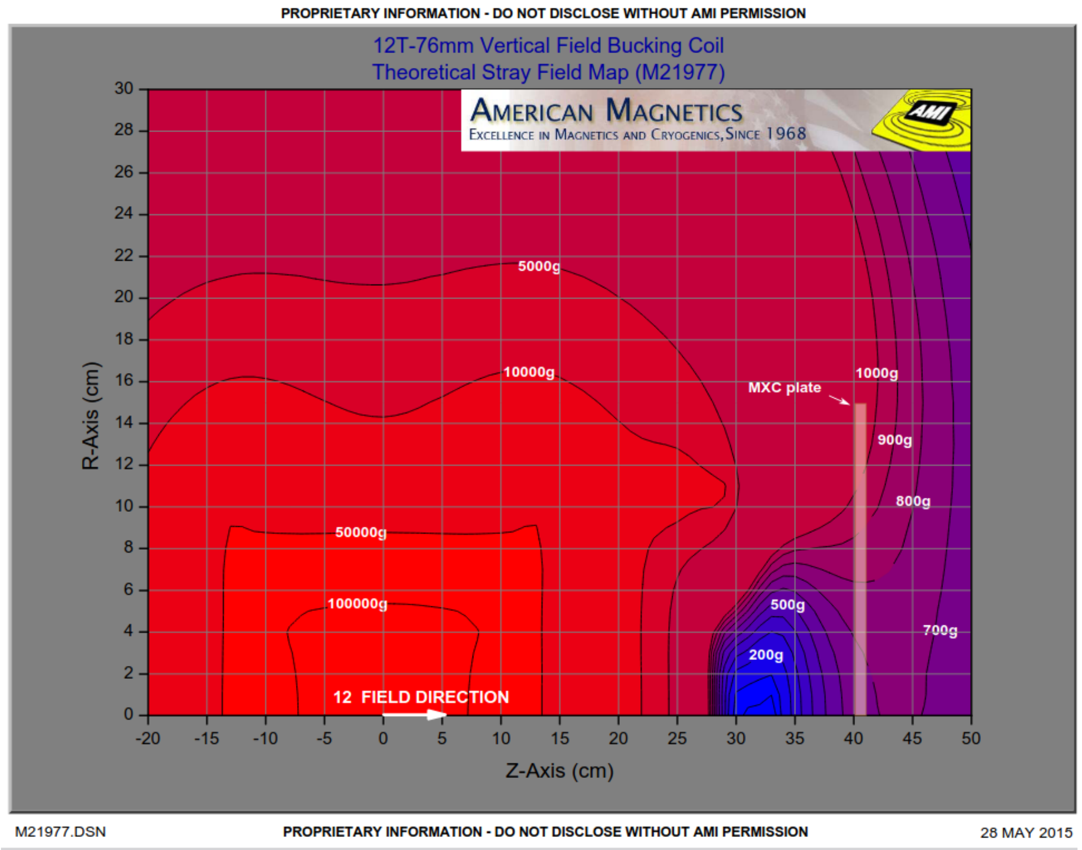

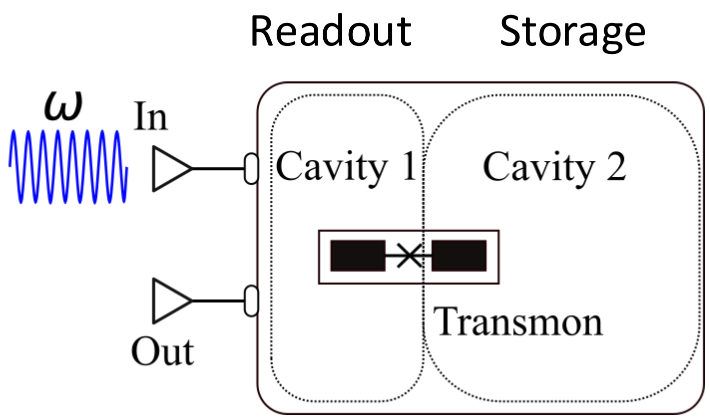

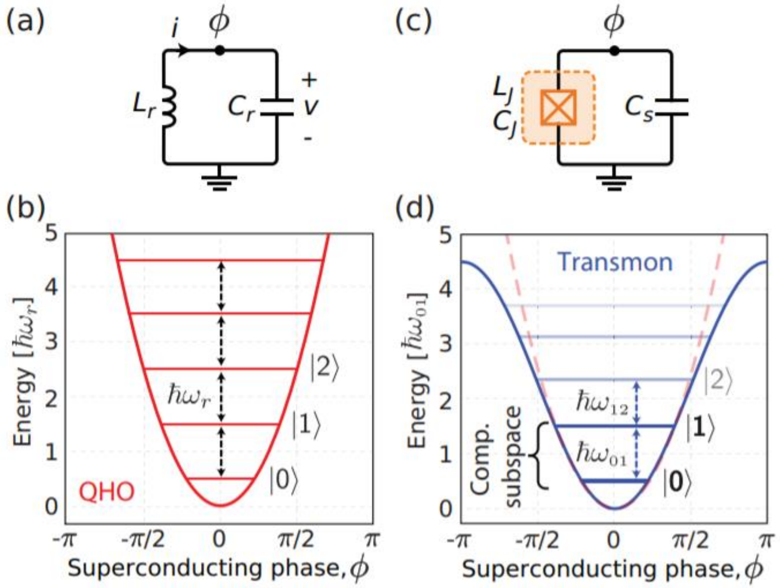

$$\hat{H}_{eff} = \underbrace{\frac{1}{2}\hbar\omega'_{01}\sigma_z}_{\text{qubit}} + \overbrace{(\underbrace{\hbar\omega'_{c1}}_{\text{cavity 1}} + \underbrace{\hbar\chi^{c1}\sigma_z)\hat{a}^\dagger\hat{a}}_{\text{Stark shift 1}}}^{\text{Readout}} + \overbrace{(\underbrace{\hbar\omega'_{c2}}_{\text{cavity 2}} + \underbrace{\hbar\chi^{c2}\sigma_z)\hat{b}^\dagger\hat{b}}_{\text{Stark shift 2}}}^{\text{Storage}}$$

$$\boxed{\chi^{c2} > \chi^{c1}}$$

Pulse sequence to inject a photon in the storage cavity

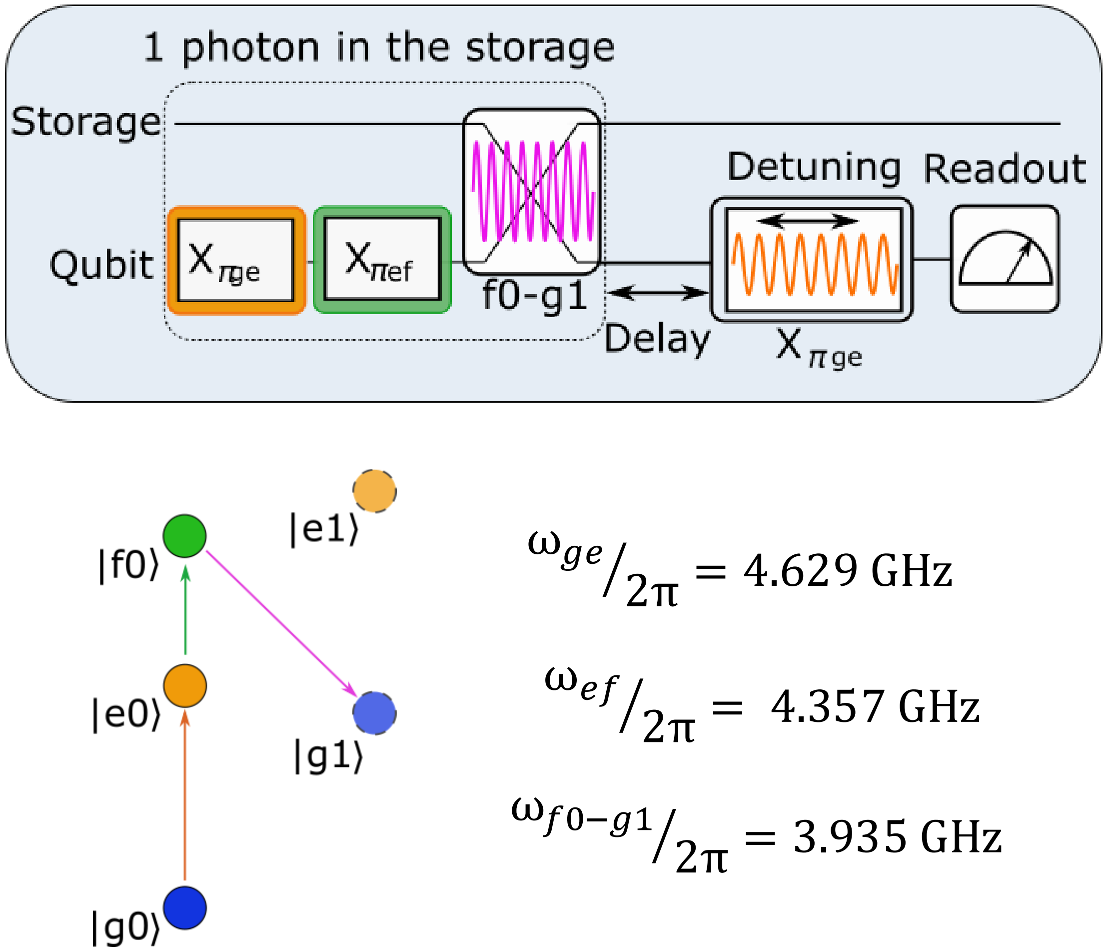

$$\omega_{ge}/2\pi = 4.629\ \text{GHz}$$

$$\omega_{ef}/2\pi = 4.357\ \text{GHz}$$

$$\omega_{f0-g1}/2\pi = 3.935\ \text{GHz}$$

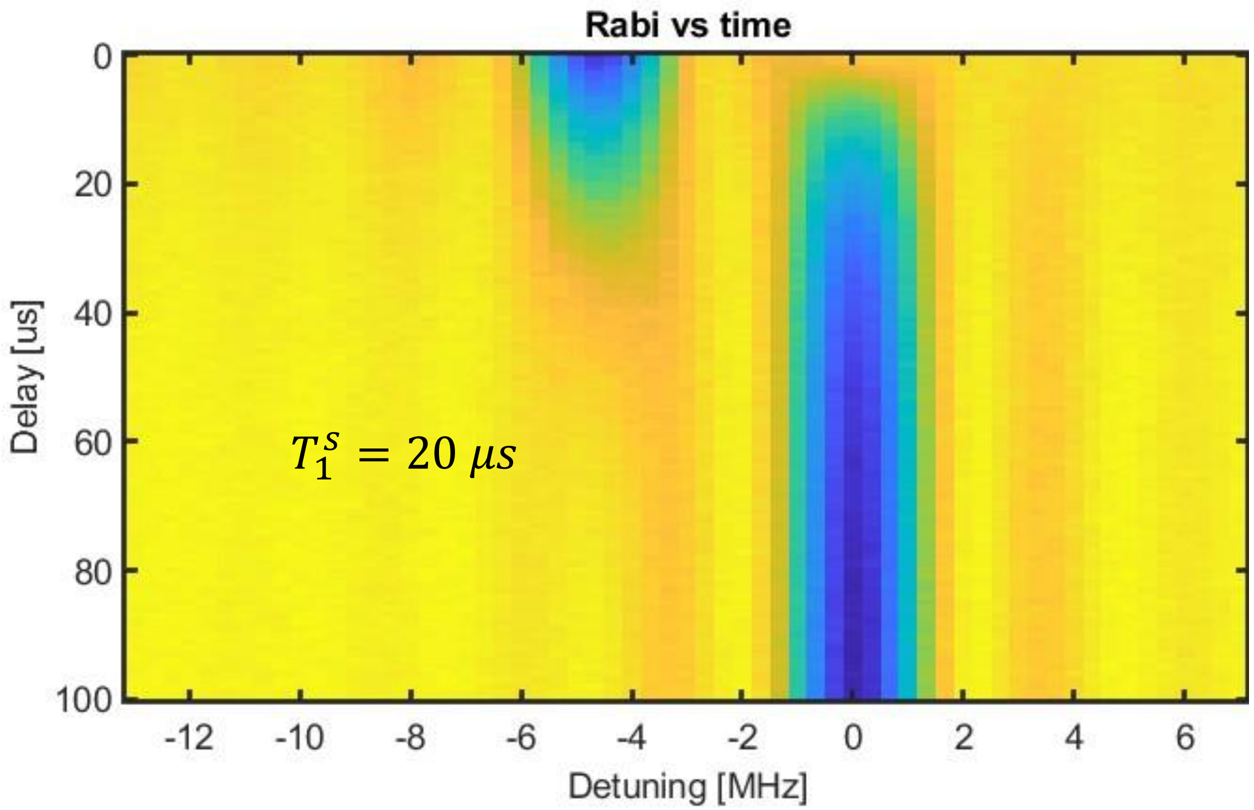

Results: counts and efficiencies

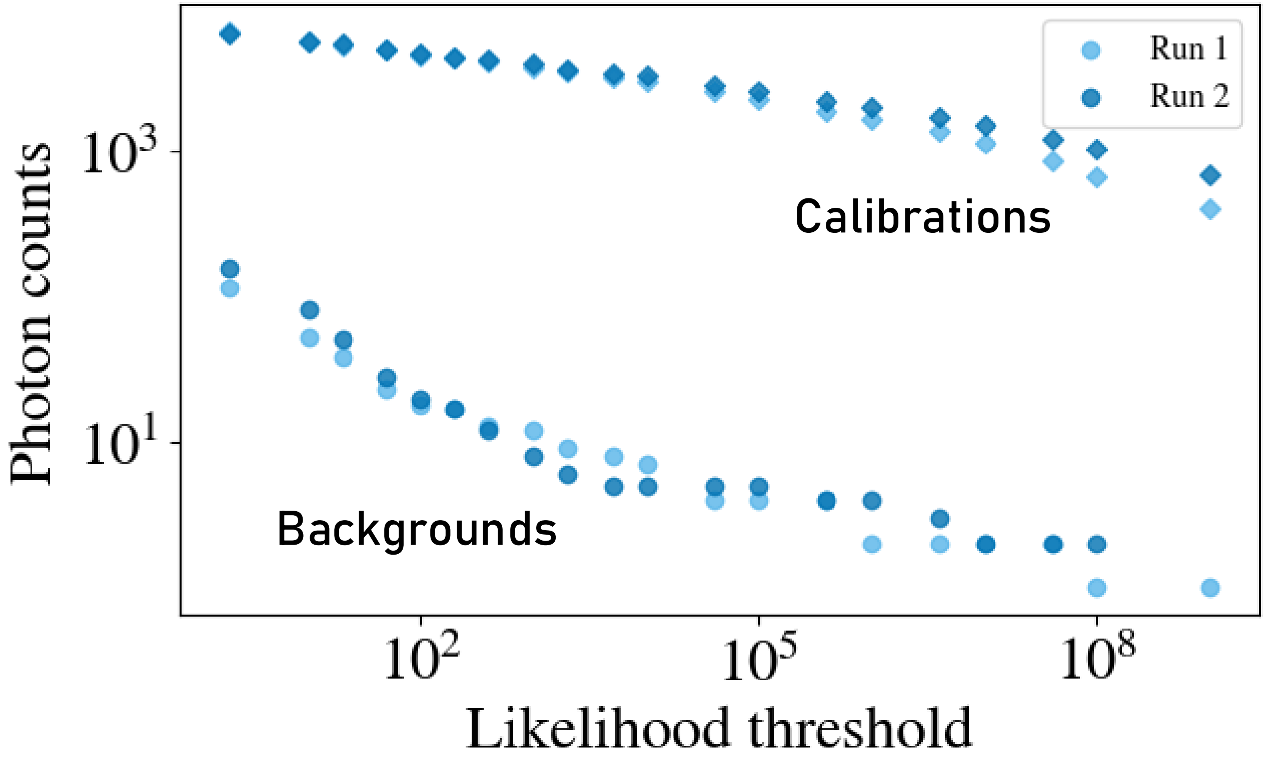

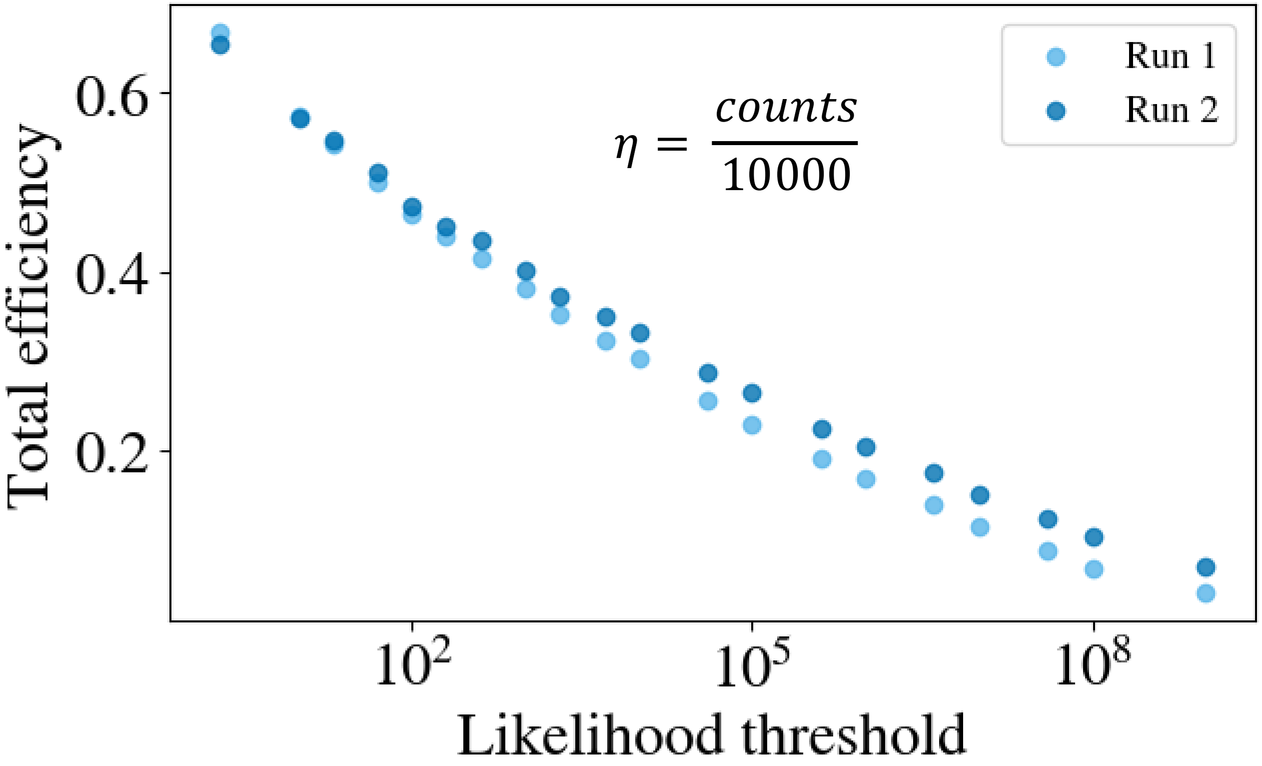

Comparison with previous works

$\lambda_{th} = 4 \times 10^4$	Background (Hz)	Efficiency	Live time (s)
Run 1	77.94	25.7%	0.2
Run 2	87.35	28.6%	0.2

Chicago group (D. Schuster)	Background (Hz)	Efficiency	Live time (s)
Searching for dark matter with a superconducting qubit	1.1	40%	8.33
A flux-tunable cavity for dark matter detection	64	15%	135201.75 (37.5 h)

Hidden Markov Model

Bayesian method to assign probabilities to each sequence.

Flat prior + forward/backward method.

Transmission matrix

$$\mathbf{T} = \begin{array}{cc} \begin{array}{cccc} |0g\rangle & |0e\rangle & |1g\rangle & |1e\rangle \end{array} & \\ \begin{bmatrix} P_{00}P_{gg} & P_{00}P_{ge} & P_{01}P_{ge} & P_{01}P_{gg} \\ P_{00}P_{eg} & P_{00}P_{ee} & P_{01}P_{ee} & P_{01}P_{eg} \\ P_{10}P_{gg} & P_{10}P_{ge} & P_{11}P_{ge} & P_{11}P_{gg} \\ P_{10}P_{eg} & P_{10}P_{ee} & P_{11}P_{ee} & P_{11}P_{eg} \end{bmatrix} & \begin{array}{c} |0g\rangle \\ |0e\rangle \\ |1g\rangle \\ |1e\rangle \end{array} \end{array}$$

Emission matrix

$$\mathbf{E} = \frac{1}{2} \begin{array}{cc} \begin{array}{cc} \mathcal{G} & \mathcal{E} \end{array} & \\ \begin{bmatrix} F_{g\mathcal{G}} & F_{g\mathcal{E}} \\ F_{e\mathcal{G}} & F_{e\mathcal{E}} \\ F_{g\mathcal{G}} & F_{g\mathcal{E}} \\ F_{e\mathcal{G}} & F_{e\mathcal{E}} \end{bmatrix} & \begin{array}{c} |0g\rangle \\ |0e\rangle \\ |1g\rangle \\ |1e\rangle \end{array} \end{array}$$

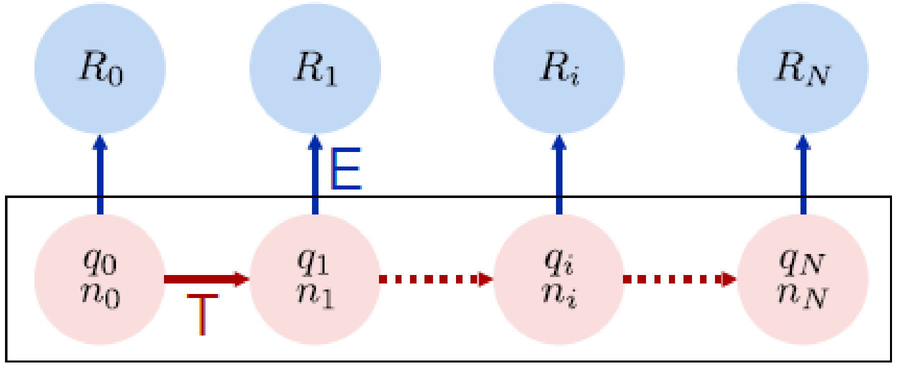

Observations
$R_i \in [\mathcal{G}, \mathcal{E}]$

Hidden states
$q_i \in [g, e]$
$n_i \in [0, 1]$

$$\begin{cases} P_{gg} = 1 - P_{ge}, P_{ee} = 1 - P_{eg} \\ P_{ge} = \bar{n}_q \left[1 - e^{-t_m/T_1^q}\right] + 1 - e^{-t_p/T_2^q} \\ P_{eg} = 1 - e^{-t_m/T_1^q} + 1 - e^{-t_p/T_2^q} \\ P^{\phi} = 1 - e^{-t_p/T_2^q} \\ P_{00} = 1 - P_{01}, P_{11} = 1 - P_{10} \\ P_{01} = \bar{n}_s \left[1 - e^{-t_m/T_1^u}\right] \\ P_{10} = 1 - e^{-t_m/T_1^u} \end{cases}$$